NASA TECHNICAL MEMORANDUM

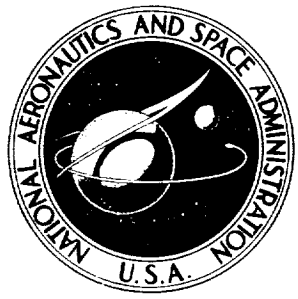

NASA TM X-3418

NASA TM X-3418

MACH 4 FREE-JET TUNNEL-STARTING EXPERIMENTS FOR A HYPERSONIC RESEARCH ENGINE MODEL CAUSING HIGH BLOCKAGE

George T. Carson, Jr., and Raymond E. Midden

Langley Research Center
Hampton, Va. 23665

NATIONAL AERONAUTICS AND SPACE ADMINISTRATION · WASHINGTON, D. C. · NOVEMBER 1976

1. Report No.	2. Government Accession No.	3. Recipient's Catalog No.
NASA TM X-3418		

4. Title and Subtitle	5. Report Date
MACH 4 FREE-JET TUNNEL-STARTING EXPERIMENTS FOR A HYPERSONIC RESEARCH ENGINE MODEL CAUSING HIGH BLOCKAGE	November 1976
	6. Performing Organization Code
7. Author(s)	8. Performing Organization Report No.
George T. Carson, Jr., and Raymond E. Midden	L-10525
	10. Work Unit No. 505-04-11-01
9. Performing Organization Name and Address	11. Contract or Grant No.
NASA Langley Research Center Hampton, VA 23665	
	13. Type of Report and Period Covered
12. Sponsoring Agency Name and Address	Technical Memorandum
National Aeronautics and Space Administration Washington, DC 20546	14. Sponsoring Agency Code

15. Supplementary Notes

16. Abstract

Tests of a full-scale hypersonic research engine (HRE) were conducted in the hypersonic tunnel facility at the Plum Brook Station of the Lewis Research Center at Mach numbers of 5, 6, and 7. Since the HRE would cause a rather high blockage (48.83 percent of the nozzle area) in the Lewis facility, subscale tests were conducted in various available small wind tunnels at Langley Research Center prior to the full-scale tests to study the effects of model blockage on tunnel starting. Presented herein are the results of the Mach 4 subscale tests which utilized a model system at 0.0952 scale which simulated the HRE in the test section of the Lewis tunnel. A satisfactory tunnel starting could not be achieved by varying the free-jet length or diffuser size nor by inserting the model into the test stream after tunnel starting. However, the installation of a shroud around the HRE model allowed the tunnel to start with the model preset in the tunnel at a tunnel-stagnation-pressure to atmospheric-exit-pressure ratio of 13.4. The simulation of the discharge of instrumentation cooling water and the addition of test hardware at the aft end of the HRE model did not have a significant effect on the tunnel starting.

17. Key Words (Suggested by Author(s))	18. Distribution Statement
Tunnel-starting experiments Hypersonic research engine	Unclassified - Unlimited Subject Category 09

19. Security Classif. (of this report)	20. Security Classif. (of this page)	21. No. of Pages	22. Price*
Unclassified	Unclassified	52	$4.25

* For sale by the National Technical Information Service, Springfield, Virginia 22161

MACH 4 FREE-JET TUNNEL-STARTING EXPERIMENTS FOR A HYPERSONIC RESEARCH ENGINE MODEL CAUSING HIGH BLOCKAGE

George T. Carson, Jr., and Raymond E. Midden
Langley Research Center

SUMMARY

Tests of a full-scale hypersonic research engine (HRE) were conducted in the hypersonic tunnel facility at the Plum Brook Station of the Lewis Research Center at Mach numbers of 5, 6, and 7. Since the HRE would result in rather high blockage (48.83 percent of the nozzle area) in the Lewis facility, subscale tests were conducted in various available small wind tunnels at Langley Research Center prior to the full-scale tests to study the effects of blockage on tunnel starting. The presently reported tests at Mach 4 utilized a 0.0952-scale model system (simulating the HRE in the test section of the Lewis tunnel) and five tunnel diffuser configurations exhausting to the atmosphere with various free-jet lengths. The HRE model was both preset in the test section and inserted from the side after the flow was established. Two pressure probes which represented less blockage than the HRE model were also used to assess tunnel starting. A meaningful test of a supersonic or hypersonic ramjet engine requires that tunnel starting be accomplished so that the impingement of any shock wave from the tunnel nozzle occurs aft of the engine inlet to avoid ingestion by the engine. This condition was not achieved by changing free-jet length and diffuser sizes.

As a second portion of the program, a shroud was installed around the HRE model. This modification required that the model be preset in the test section. The shroud enabled the tunnel to

start at a stagnation-pressure to atmospheric-exit-pressure ratio of 13.4. A ring, called an adverse-pressure-gradient barrier, was added at the front of the shroud to inhibit reverse flow from the shroud into the test section. This addition resulted in a small (1 percent) reduction in tunnel-starting stagnation pressure but apparently had a favorable effect in reducing the test-section static pressure. The aft end of the HRE model was modified to simulate the addition of test hardware used intermittently on the full-scale test engine. These additions were instrumentation cooling water and an airflow metering duct. These items did not significantly affect the tunnel starting.

INTRODUCTION

Tunnel-blockage problems need to be evaluated in order to minimize the size of supersonic wind tunnels using heated, high pressure air and while maximizing the size of the models to be tested. These problems are not usually amenable to analytic solution and, generally, experimentally derived solutions are sought.

Prior to tests (refs. 1 and 2) of a hypersonic research engine (a supersonic combustion ramjet or scramjet) in the hypersonic tunnel facility (HTF) at the Plum Brook Station of the Lewis Research Center, subscale (about one-tenth) tests were conducted at Langley Research Center utilizing existing small-scale facilities. The full-scale hypersonic research engine (HRE) tested in the HTF resulted in a tunnel blockage (model area projected on the tunnel-nozzle exit area) of about 49 percent when in the test position. Subscale tests were conducted at Mach numbers of 4, 5, and 7 to cover the expected test range for the full-scale HRE. The Mach 5 subscale tests (ref. 3) were conducted in a relatively low-temperature (534 K) airflow using many of the configurations of the present investigation, but were made with a vacuum exhaust system. The use of air ejectors at the exit of the tunnel nozzle and ahead of the diffuser inlet was explored with some favorable results;

however, the air ejectors were not included in the presently reported Mach 4 tests. The Mach 7 tests were conducted in much the same manner as the Mach 4 tests but with a vacuum exhaust system. The Mach 7 results have not been formally reported.

The tunnel-model-diffuser arrangement used is generally typical of heated, high-pressure, free-jet facilities. Therefore, these results are considered of interest in areas other than the testing of hypersonic propulsion systems.

The purpose of these Mach 4 experiments may be considered in three parts: first, to determine the starting capability of the HTF with the HRE model installed; second, to determine the modifications required in order to obtain starting; and third, to provide quantitative relationships, such as pressure ratios, required for starting of different configurations.

Tests were conducted in the 11-inch ceramic-heated tunnel (CHT) using a 0.0952-scale model of the HRE with an existing Mach 4 tunnel nozzle. The HTF test cell and tunnel diffuser were simulated at about the proper scale. The tunnel was operated at various stagnation pressures from 7 to 34 atm and at approximately true Mach 4 flight stagnation temperature (880 K). There was actually a variation in tunnel stagnation temperature from 644 K to about 889 K depending on the ceramic-bed temperature. This variation was not considered to have a significant effect. The test unit Reynolds number at the highest stagnation pressure was about three times the Lewis HTF unit Reynolds number.

SYMBOLS

A area, cm^2

D diameter, cm

d location of pressure tap at end of diffuser

L free-jet length

M	Mach number
N_{Re}	unit Reynolds number, m^{-1}
p	pressure, atm (1 atm = 101 325 Pa)
q	dynamic pressure, Pa
s	location of pressure tap at test section
T	temperature, K
V	velocity, m/s
γ	ratio of specific heats

Subscripts:

d	diffuser
e	exit
n	tunnel-nozzle exit
s	test section
t	total
t,1	plenum heat exchanger, stagnation conditions
∞	free stream
1 to 9	pressure taps at locations shown in figure 7

MODELS, APPARATUS, AND TESTS

Models

The primary blockage test item used in this program was a 0.0952-scale solid model of the HRE in the inlet-closed configuration. Figure 1 is a quarter view of this model and figure 2 gives the assembly dimensions and shows components which are referred to in this paper. The solid HRE model was used to give what was considered a conservative evaluation of the tunnel blockage. The model maximum external surface angle of 37° to the tunnel center line occurred on the cowl section just aft of the inlet-spike section. From simple analysis and the HRE inlet test data of reference 4, turning of the entire tunnel flow around the model was judged to result in more shock loss (more conservative condition) than allowing some flow to go through the engine during tunnel starting. Two other blockage test items were used to a much lesser extent. They were a pitot pressure probe 1.27 cm in diameter with a hemispherical nose causing 8.52-percent blockage and a conical pitot probe 5.08 cm in diameter with a 60° conical (including angle) nose causing 33-percent blockage.

The HRE model, including the two mounting struts, represented a blockage, based on projected area, or 48.83 percent of the nozzle area of the 11-inch ceramic-heated tunnel. Figure 3 shows percentage of total blockage for various models tested in the 11-inch CHT at Mach numbers of 4 and 6. The Mach 6 information was obtained from reference 5.

Apparatus

The 11-inch ceramic-heated tunnel used in this program is described in reference 5. Briefly, this facility consists of a high-pressure air supply, a gas-burner-heated ceramic-element (0.9525-cm-diam. spheres) plenum heat exchanger, a 10.16-cm-diameter water-cooled Mach 4 nozzle, a free-jet test section,

and a diffuser (of which five configurations were tested). The facility name originates from the size of the nozzle attachment flange (i.e., 11-in. (27.94 cm)). The photograph of figure 4 shows the HRE model in the test section. The bolt head in the tunnel nozzle exhaust plane should be noted since it appears in the shadowgraph figures. The test apparatus included an electropneumatic mechanism to swing models into the test stream from the side in a manner such that the center line of the models remained parallel with the center line of the tunnel nozzle. The sketch of figure 5(a) indicates the HRE model position in relation to the nozzle diffuser and viewing port when fixed in the free jet, and figure 5(b) indicates the position of the model when inserted from the side after tunnel starting. The free-jet length, which is varied, is shown in figure 5 and is defined as the distance between the exit of the tunnel nozzle and the inlet to the diffuser. With a shroud around the model, the free-jet length was considered to be the distance between the nozzle exit and the front of the shroud.

The diffuser configurations used in the initial part of this program are shown in figure 6. Diffuser configurations 1, 2, and 3 represented a diffuser straight-pipe section of cross-sectional area 1.15 times the tunnel-nozzle exit area which was the same area ratio as existed in the HTF for the full-scale engine. The ratios of diffuser area to nozzle area of configurations 4 and 5 increased to values of 1.35 and 1.59, respectively. These area ratios were achieved by using two standard size tubes which bracketed the maximum possible increase in full-scale HTF diffuser to nozzle area ratio of 1.53. The length of the straight section of the diffuser was set at about 10 diffuser diameters for configuration 1 which represented the full-scale design. This length was held constant for the other configurations. For the second part of the program a shroud, consisting of a steel shell welded to the struts, was installed around the HRE model. Later in the test program a ring was added to the front of the shroud to provide a smaller entrance diameter to the shroud and to provide a step on the inside to decrease the reverse flow caused by the adverse pressure gradient on the inside of the

shroud. This resulted in the designation adverse-pressure-gradient barrier for the ring. For this part of the program, diffuser configurations 1, 4, and 5 were used with a diverging section added to the downstream end of each diffuser. A pitot pressure rake was located at the end of the constant area duct as noted in figure 7.

Tests

The test environment for the presently reported experiments in the 11-inch CHT was controlled to simulate the Lewis HTF, which in turn duplicated the HRE design flight test condition at Mach 4 (a flight dynamic pressure of 86.18 kPa). Table 1 shows the Mach 4 flight environment for the HRE. Table 2 shows the comparison of several basic aerothermodynamic input values between the Mach 4 tests in the HTF and the 11-inch CHT. The Reynolds numbers shown were calculated using the values of this table and relationships given in reference 6. It is noted that the unit Reynolds number of the present experiment was about three times the unit Reynolds number of the HTF, although the scale of the model for the experiments was about one-tenth size.

The procedure for operating the facility was to increase the stagnation pressure in steps to a maximum of 34 atm since this is the estimated maximum pressure of the HTF at Mach 4. For those tests where the model position was fixed in the tunnel nozzle, the tunnel configuration was considered unsatisfactory if the tunnel could not be started and operated with a total pressure of 34 atm. For those tests in which the model was inserted into the established flow, if the tunnel became unstarted, the model was retracted and the stagnation pressure increased. The model was again inserted. This procedure was followed until the minimum starting stagnation pressure could be defined or until it was shown that starting could not be obtained within the required 34-atm pressure limit.

Measurements and Accuracy

During each test of the initial part of the program, measurements of stagnation pressure and test-section static pressure were made. Also, shadowgraph photographs of the flow were obtained using a 16-mm motion-picture camera operating at 128 frames per second. During each test of the second part of the program, similar data were taken as well as static pressures on the inner top longitude of the shroud and pitot pressure profiles at the end of the constant-area section of the diffuser.

For the 11-inch CHT, as discussed in reference 5, the temperature of the top of the pebble bed as read by an optical pyrometer is used to determine the stagnation temperature. However, the stagnation temperature required for these tests was near the lower limit of the operating range of the pyrometer. In order to verify the stagnation-temperature measurements, a chromel-alumel, choke-vented-stagnation-cup thermocouple probe was installed in the exit of the tunnel nozzle. Reference 7 discussed the accuracy of this type of probe as having a probable error of 0.7 percent of the stagnation temperature.

Reference 6 states that the accuracy of the other required flow parameters are within the following limits:

M	± 0.12
$p_{t,1}$, atm	1.36
p_s, atm	± 0.02

Diffuser exit pressure p_e was assumed to be atmospheric and set as $p_e = 1$ atm for all calculations.

RESULTS AND DISCUSSION

The changes in tunnel-model configuration were related to an assessment of what blockage was allowed in the test stream with a given tunnel diffuser and to feasible changes in the existing HTF

equipment in order to allow the tunnel to start and operate with the HRE in the test position. Besides the changes in tunnel-diffuser configuration, the addition of a shroud around the model was a major configuration change. Other variables evaluated were insertion of the models into the test stream, changes to the shroud, and changes to the HRE model to simulate the addition of test hardware which would be used during the full-scale test program.

Effect of Diffuser Configuration on Tunnel-Starting Characteristics

The test setups, including changes in diffuser configuration and free-jet length, and the associated tunnel-flow starting stagnation pressure ratios are summarized in part 1 of table 3. Some unsuccessful tests will not be discussed in detail. The results for each of the five variations in diffuser configuration are discussed in the following sections.

Diffuser configuration 1.- Diffuser configuration 1 with dimensions as shown in figure 6 was installed and tests were conducted with the test section empty and then containing, first, a 1.27-cm-diameter hemispherical pitot pressure probe and, finally, the HRE model. Figure 8 is a shadowgraph showing the pitot probe in the free jet with the tunnel started. Figure 9 shows the HRE model in the free jet. The tunnel did not start with the model in the test section.

When the tunnel started, the test-section static pressure would descend to a low minimum value and remain below the diffuser exit pressure for even high stagnation pressure. This trend may be seen in figure 10 which shows the variation of test-section static pressure with plenum stagnation pressure for diffuser configuration 1. It is noted from figure 10 that the trend of the test-section pressure was not the same with the HRE model in the test position as with the 1.27-cm-diameter probe; although there is a relatively sharp break at $p_{t,1}/p_e \approx 15$. The rise in test-section static pressure beyond $p_{t,1}/p_e = 16$, along with

the shadowgraphs taken during the testing, indicated the tunnel was not started. (Note: Pressures given in the figures have been nondimensionalized by the exit pressure.)

Diffuser configuration 2.- After tunnel starting could not be achieved with the HRE model in the test section, the diffuser inlet diameter was increased as shown in figure 6, configuration 2, in order to capture a larger mass flow. Figure 11 shows the test-section static pressure for diffuser configuration 2. The same trend of low test-section pressure is shown for the tunnel-model configurations which started or remained started after model insertion as was shown for diffuser configuration 1. For the test section empty, the effect of shorter free-jet length was to reduce the test-section static pressure. The tunnel started easily while the test section was empty or contained the 1.27-cm-diameter pressure probe. Next, a 5.08-cm-diameter conical pitot pressure probe with a 60° apex angle, resulting in a 33-percent blockage, was installed in the test section and the tunnel would not start. Figure 12 is a shadowgraph of this probe in the unstarted tunnel. Using the electropneumatic mechanism, the 1.27-cm pitot pressure probe was inserted into the free jet after the flow was established. The tunnel remained started and the test-section static pressure p_s corresponding to any stagnation pressure $p_{t,1}$ was less than that obtained (not shown in fig. 11) for the probe in the fixed position for the same free-jet length. This technique was applied to a test run with the HRE model. However, when the model was inserted, the tunnel unstarted immediately. The disturbed flow pattern caused by the HRE model may be seen in figure 13.

Diffuser configuration 3.- The next step was to extend the diffuser inlet as shown in figure 6 (configuration 3). The idea was to capture enough of the flow around the HRE model to effect tunnel starting. However, this scheme offered no advantages as may be seen in figure 14.

Diffuser configuration 4.- The results using diffusers 1, 2, and 3 indicated that a larger diffuser might be necessary to enable the tunnel to start with the HRE model in the test section.

Figure 15 shows the test-section static pressure as a function of plenum stagnation pressure for the test section empty and containing the HRE model at two different free-jet lengths for diffuser configuration 4. Tunnel starting was not achieved with the HRE model using this configuration.

Diffuser configuration 5.- The largest diffuser (configuration 5) was tested with the test section empty, 1.27-cm-diameter pitot probe both fixed and inserted, HRE model fixed with a short free-jet length, HRE model inserted, and HRE model inserted with one strut removed. The test-section static pressure is presented in figure 16. The tunnel still could not be started with the HRE model in the test section. There is no apparent effect of free-jet length on starting with the 1.27-cm pressure probe. With the tunnel empty, the test-section pressure was lower with the shorter free-jet length.

Effect of Shroud on Tunnel-Starting Characteristics

The test setups, which utilized a shroud around the model, are summarized in table 3. The diffuser size was varied and test hardware and water discharge (simulating instrumentation cooling) were added to assess the effects on tunnel starting. These results are discussed in the following sections.

Diffuser configuration 1.- Diffuser configuration 1 with dimensions as shown in figure 6 and arranged as shown in figure 7 represented the planned modification to the HTF. Figure 17 is a photograph of the HRE model with the shroud installed in the test section. It should be noted that for the first tests, the adverse-pressure-gradient barrier was not installed on the front of the shroud. More detail of the shrouded HRE model may be seen in figure 18. Figure 19 is a shadowgraph of the HRE model with shroud and the tunnel started. The shadowgraph of this configuration is the only one presented, since the shadowgraphs of all subsequent shrouded configurations appear basically the same. It is noted from the shadowgraph that there are shock waves coming from the

end of the tunnel nozzle. The existence and strength of these shock waves are determined by the pressure rise required at the nozzle exit to match the test-section pressure along the bounding streamline. Because of this, the level of the test-section pressure is a limiting criterion in the determination of the acceptability of the started condition of the tunnel flow. From figure 20, which shows the variation of test-section pressure with stagnation pressure, it can be seen that the test-section pressure reached a minimum of about 0.2 at a stagnation pressure of 13.4, which indicated tunnel starting. The nozzle static pressure ratio p/p_e is 0.087 at a stagnation pressure ratio of 13.4, which indicates a pressure rise (0.2 divided by 0.088) of 2.25 across the shock waves seen in figure 19. This pressure rise at the end of the Mach 4 nozzle would imply little or no boundary-layer separation within the nozzle. Also, since the shock waves impinge on the HRE model aft of the cowl leading edge, this starting condition was considered satisfactory, at least at the front of the model, for full-scale testing in HTF.

In principle, the addition of the shroud to the model captured the flow out of the tunnel nozzle and directed it around the model. At the same time, because of mixing along the free-jet boundary, some of the quiescent air in the test section is entrained and pumped into the shroud. Within the shroud the flow expands supersonically into the large area behind the model to a static pressure which is low enough, with mixing aft of the shroud within the diffuser inlet, to induce added flow from the test section through the annular slot between the shroud and the diffuser inlet. It was considered that the nearer the test-section pressure approached the nozzle-exit static pressure, the better the tunnel-starting condition. The annular slot with diffuser 1 (diffuser straight-section area 15 percent greater than nozzle area) did limit the minimum value of test-section pressure to about twice the nozzle-exit static pressure at Mach 4 (fig. 20) and Mach 5 (ref. 3). The unpublished results of the Mach 7 tests indicated reverse flow through the annulus was possible at some times during starting and that the

minimum test-section pressure was about twice the nozzle-exit static pressure.

Since the tests of reference 3 had indicated that sealing the shroud to the struts was an important factor in keeping the tunnel started, the Mach 4 HRE model and shroud were sealed along the mounting struts by welding. When tested, this sealing around the struts had no apparent effect on the test-section pressure as shown in figure 20 or on the diffuser-exit static pressure shown in figure 21.

The testing of ramjet or scramjet engines usually involves water-cooled instrumentation probes in the engine exit flow and other hardware at the exit. For the HRE tests, there was concern that these additions would result in adverse effects on tunnel starting or the test-section pressure and that evaluation of the effects was needed. To simulate the mass flow and approximate distribution of the instrumentation cooling water discharged aft, a tube was bent in a "V" shape to follow roughly the exit lines of the HRE from the outside of the engine nozzle to the apex of the nozzle plug and back to the outside of the engine nozzle. The tube was routed behind the HRE model support strut to limit the flow interference. This arrangement is shown in figure 22. The water mass flow rate (0.136 kg/s) was about 10 percent of the airflow rate at a tunnel stagnation pressure of 13.4 atm. The presence of the tube without water discharge caused an increase of about 1 percent, as can be seen from the data of part 2 of table 3, in the starting stagnation pressure ratio (up from 13.4 to 13.6). With the water discharge from the tube, the starting stagnation pressure ratio was reduced about 3 percent (down from 13.6 to 13.2).

In an effort to lower the required starting stagnation pressure ratio, a ring-shaped adverse-pressure-gradient barrier shown in figure 7 was added to the leading edge of the shroud. The nature of the barrier is apparent by comparison of figures 18 and 23. The barrier did have a slightly beneficial effect in reducing the tunnel-starting pressure ratio (i.e., 13.4 and 13.0,

without and with water discharge, respectively). The barrier's primary effect was to smooth the test-section static pressure as may be seen in comparing figure 24 with figure 20. Furthermore, the addition of the barrier along with the other effects resulted in a test-section pressure which was only 1.5 times the nozzle-exit static pressure at a tunnel stagnation pressure of 13 atm. Included in figure 24 is the variation of shroud static pressure with plenum stagnation pressure for several pressure-tap locations shown in figure 7.

The addition of the adverse-pressure-gradient barrier, which gave a satisfactory test condition, resulted in the relatively low test-section static pressure (about 1.5 times the nozzle-exit static pressure) shown in figure 24. The other critical area was at the HRE model nozzle exit station. Here the static pressure in the flow surrounding the model must not be so high as to cause a shock wave across the engine-nozzle flow which either separated the engine-nozzle internal flow or impinged on the engine nozzle plug to alter the nozzle pressure distribution. At Mach 4, it was determined from analysis of the engine-nozzle flow that the external static pressure on the HRE model at the nozzle exit station would be acceptable if the value was 2.5 times the tunnel-nozzle-exit static pressure. Figure 24 indicates that at stagnation pressure ratios from 13.4 to about 15.4, this condition would be met if p_2/p_e on the model shroud was used as an index. Since there is some expansion around the base of the HRE model, as indicated in figure 24, the static pressure at the HRE-model-nozzle-exit station was judged to be probably lower than at the location of p_2 on the model shroud. Figure 25 shows the corresponding variation of diffuser static and pitot-rake pressure with plenum stagnation pressure for the static-pressure-tap and pitot-rake locations shown in figure 7.

A section of constant diameter was added to the aft end of the HRE model, as shown in figure 26, to simulate the outer contour only of an airflow metering device which was to be used in the full-scale tests to measure engine airflow. The effect of

this addition in model volume (no change in model length) was unpredictable from analysis. The variation of the test-section and shroud static pressure with stagnation pressure with the simulated airflow metering device added is shown in figure 27. When comparing figure 20 with figure 27, a small reduction in the starting stagnation pressure might be expected, as previously noted, because of the addition of the adverse-pressure-gradient barrier, but the starting stagnation pressure was slightly higher (about 13.6 compared with 13.4) evidently because of the addition of the simulated airflow metering duct. It was noted that the test-section static pressure remained low at about 1.5 times the tunnel-nozzle-exit static pressure. It is speculated that the adverse-pressure-gradient barrier reduced reverse flow out the front of the shroud, which allowed the test-section pressure to remain at the low level attained. The nozzle shroud and HRE model external surface pressures were not critical for the setup using the airflow metering device. For this arrangement, the erratic variation of the pressure data is apparently due to the reflection and interaction of shock waves. The corresponding variation of diffuser static and pitot-rake pressure with plenum stagnation pressure for this arrangement is shown in figure 28.

Diffuser configuration 4.- As done previously without the shroud, the effect of diffuser cross-sectional area was investigated. Figure 29 shows how the test-section static pressure varied with plenum stagnation pressure for the test setup including diffuser configuration 4, which has a diffuser area to tunnel-nozzle area ratio of 1.35 compared with 1.15 for the existing HTF. A comparison of this figure with figure 27 shows that no benefit in starting stagnation pressure is obtained from the larger diffuser; and in fact, the test-section pressure is somewhat higher at the same started stagnation pressure, even though the free-jet length was reduced to equal the tunnel-nozzle diameter.

Diffuser configuration 5.- Diffuser configuration 5 had the largest ratio of diffuser area to tunnel-nozzle area (i.e., 1.59). Figure 30 shows how the test-section static pressure varied with

plenum stagnation pressure for the same test setup. By comparing this figure with the previous figure the increased area ratio is seen to be detrimental since the starting pressure required was increased to 15.4.

As additional information, it is noted that reference 3 describes an experimental program conducted at Mach 5 for a simulated HTF and HRE model. An additional aspect of these experiments was the use of annular ejector nozzles, one located at the end of the Mach 5 nozzle and one at the entrance to the diffuser, which slightly improved starting characteristics. In this experiment, supersonic flow could be maintained by inserting the HRE model into an already established stream.

CONCLUDING REMARKS

Tests of a full-scale hypersonic research engine (HRE) were conducted in the hypersonic tunnel facility at the Plum Brook Station of the Lewis Research Center. The Mach numbers of the test program were 5, 6, and 7. Since the HRE would result in a rather high blockage (48.83 percent of the nozzle area) in the Lewis facility, subscale tests were conducted in various available small wind tunnels at the Langley Research Center prior to the full-scale tests. The present report is concerned with Mach 4 subscale tests, which were conducted at a stagnation temperature of 880 K and at stagnation pressures up to 34 atm.

In order to study the effects of blockage on tunnel starting at Mach 4, a 0.0952-scale model simulating the HRE in the test section of the Lewis full-scale tunnel was used with five diffuser configurations at various free-jet lengths. In these subscale tests, the ratio of the design diffuser cross-sectional area to tunnel-nozzle-exit area was 1.15, with a diffuser straight-pipe section about 10 diffuser diameters in length. The diffuser exhausted to the atmosphere and the tunnel-starting stagnation pressure ratio was determined by the value of the tunnel stagnation pressure in atmospheres when satisfactory tunnel starting

was achieved. During this investigation, the HRE model was tested both preset in the test section and inserted from the side after supersonic flow had been established. In order to test a ramjet or scramjet engine with an inlet in a supersonic stream, it is required that tunnel starting be accomplished so that the impingement of any shock waves from the tunnel nozzle occurs downstream of the engine inlet to avoid ingestion by the engine. It is also required that the static pressure near the engine nozzle be low enough so as not to influence the nozzle pressure distribution and, thereby, the engine thrust.

During the first portion of the test program, a satisfactory tunnel-started condition could not be achieved with the HRE model by altering the diffuser entrance geometry, by increasing the diffuser area by 33 percent, or by injecting the HRE model into the stream after the tunnel had started empty. Tunnel starting was possible using a pitot probe which resulted in about 8.52-percent tunnel blockage but was not possible with a second probe at about 33-percent blockage.

During the second portion of the program, a shroud was installed around the HRE model (which required that the model be preset in the test section) and satisfactory tunnel starting was achieved at a tunnel stagnation pressure of 13.4 atm. Although the addition of a water tube aft of the model increased the tunnel-starting stagnation pressure about 1 percent, the downstream discharge of water simulating full-scale instrumentation cooling (water mass flow about 10 percent of tunnel airflow) gave a subsequent reduction of about 3 percent in tunnel-starting stagnation pressure. A ring, called an adverse-pressure-gradient barrier, was installed at the front of the shroud reducing the shroud entrance area and providing a step to inhibit reverse flow from the inside of the shroud. This addition caused a 1-percent reduction in starting stagnation pressure and the test-section static pressure was about 1.5 times the tunnel-nozzle static pressure. The addition of volume (constant diameter) to the aft end of the HRE model to simulate full-scale hardware gave a

1-percent increase in tunnel-starting stagnation pressure but, after starting, the test-section pressure remained at about 1.5 times the tunnel-nozzle-exit static pressure. Changes to diffusers of 17 and 33 percent larger area gave no adverse effects on the tunnel-starting stagnation pressure level.

Langley Research Center
National Aeronautics and Space Administration
Hampton, VA 23665
August 13, 1976

REFERENCES

1. Andersen, W. L; and Kado, L.: Hypersonic Research Engine Project - Phase II. Aerothermodynamic Integration Model (AIM) Test Report. NASA CR-132655, 1975.
2. Engineering Staff: Hypersonic Research Engine Project - Phase II. Aerothermodynamic Integration Model Development. Final Technical Data Report. NASA CR-132654, 1975.
3. Molloy, John K.; Mackley, Ernest A.; and Keyes, J. Wayne: Effects of Diffusers, Shrouds, and Mass Injection on the Starting and Operation Characteristics of a Mach 5 Free-Jet Tunnel. NASA TN D-6377, 1971.
4. Pearson, L. W.: Hypersonic Research Engine Project - Phase IIA. Inlet Program. Final Technical Data Report. AP-69-4883 (Contract No. NAS 1-6666), AiResearch Manufacturing Company, Mar. 27, 1969. (Available as NASA CR-66797.)
5. Midden, Raymond E.; and Cocke, Bennie W., Jr.: Diffuser Performance of a Mach 6 Open-Jet Tunnel and Model-Blockage Effects at Stagnation Temperatures to 3,600° F. NASA TN D-2384, 1964.
6. Ames Research Staff: Equations, Tables and Charts for Compressible Flow. NACA Rep. 1135, 1953. (Supersedes NACA TN 1428.)
7. Glawe, George E.; Simmons, Frederick S.; and Stickney, Truman M.: Radiation and Recovery Corrections and Time Constants of Several Chromel-Alumel Thermocouple Probes in High Temperature, High Velocity Gas Streams. NACA TN 3766, 1956.

TABLE 1.- MACH 4 FLIGHT ENVIRONMENT FOR HRE

Flight condition	Altitude, m	p_∞, atm	T_∞, K	$p_{t,\infty}$, atm	$T_{t,\infty}$, K	q_∞, Pa	V_∞, m/s
Design	17 983	0.075	217	13.479	880	84 796	1180
4572 m above design	22 555	.037	219	5.705	890	41 560	1187
Maximum dynamic pressure	17 069	.086	217	11.572	880	97 819	1180

TABLE 2.- COMPARISON OF SEVERAL BASIC AEROTHERMODYNAMIC INPUT VALUES BETWEEN THE HTF AND THE 11-INCH CHT MACH 4 TESTS

Input parameter	HTF	11-inch CHT
M_∞	4.0	4.0
$T_{t,\infty}$, K	880.0	880.0
$p_{t,\infty}$, atm	11.57	30.91
$p_t/p_{t,\infty}$	30.91	30.91
D_{HRE}, cm	70.56	6.72
N_{Re}, m^{-1}	11.713×10^6	31.306×10^6

TABLE 3.- SUMMARY OF TEST PROGRAM

Test subject	L/D_n	Diffuser configuration	A_d/A_n	Tunnel-starting pressure ratio
Without shroud				
Empty test section	[a]1.55	1	[a]1.15	9.33
Pitot probe, 1.27-cm diameter	[a]1.55	1	[a]1.15	14.33
HRE	[a]1.55	1	[a]1.15	(d)
Empty test section	[a]1.19	2	[a]1.15	9.33
Pitot probe, 5.08-cm diameter	1.03	2	[a]1.15	(d)
HRE	1.19	2	[a]1.15	(d)
HRE	.45	2	[a]1.15	(d)
Empty test section	[b]2.17	2	[a]1.15	11.00
Pitot probe (inserted), 1.27-cm diameter	[b]2.17	2	[a]1.15	14.33
HRE (inserted)	[b]2.17	2	[a]1.15	(d)
HRE	.45	3	[a]1.15	(d)
Empty test section	1.00	4	[c]1.35	11.67
HRE	1.00	4	[c]1.35	(d)
HRE	[b]2.17	4	[c]1.35	(d)
Empty test section	1.53	5	[c]1.59	13.00
Pitot probe (inserted), 1.27-cm diameter	1.53	5	[c]1.59	14.33
HRE	1.53	5	[c]1.59	(d)
Empty test section	2.35	5	[c]1.59	13.00
HRE (inserted)	2.35	5	[c]1.59	(d)
HRE	1.00	5	[c]1.59	(d)
HRE (inserted)	[b]2.17	5	[c]1.59	(d)
HRE (one strut; inserted through cut out)	1.97	5	[c]1.59	(d)
HRE (one strut)	1.00	5	[c]1.59	(d)
With shroud				
HRE (shroud)	[a]1.55	1	[a]1.15	13.40
HRE (shroud, S)	[a]1.55	1	[a]1.15	13.40
HRE (shroud, S, W_o)	[a]1.55	1	[a]1.15	13.60
HRE (shroud, S, W_1)	[a]1.55	1	[a]1.15	13.20
HRE (shroud, S, W_o, B)	[a]1.55	1	[a]1.15	13.40
HRE (shroud, S, W_1, B)	[a]1.55	1	[a]1.15	13.00
HRE (shroud, S, B, A)	[a]1.55	1	[a]1.15	13.60
HRE (shroud, S, B, A, I_6)	[a]1.55	1	[a]1.15	14.80
HRE (shroud, S, B, A, I_4)	[a]1.55	1	[a]1.15	14.00
HRE (shroud, S, B, A, I_6)	1.00	4	[c]1.35	14.00
HRE (shroud, S, B, A)	1.00	4	[c]1.35	13.60
HRE (shroud, S, B, A)	1.00	5	[c]1.59	15.40

[a]Original HTF design geometric ratios.

[b]Based on minimum FJL for HRE injection.

[c]Based on maximum possible HTF diffuser diameter.

[d]Never started or for the model inserted cases the tunnel unstarted.

Notation:

S Sealed around shroud-strut joint.

W_o Instrumentation cooling water system, not flowing.

W_1 Instrumentation cooling water system, flowing.

B Adverse-pressure-gradient barrier.

A Airflow metering duct.

I_6 Instrumentation struts, 6 installed.

I_4 Instrumentation struts, 4 installed.

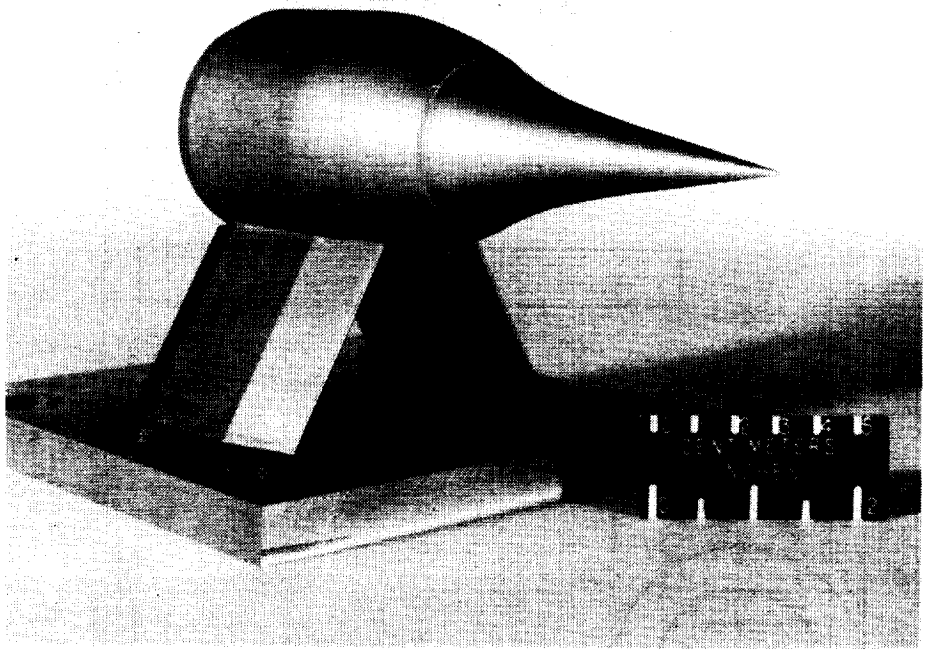

L-76-437

Figure 1.- Quarter view of the 0.0952-scale model of the hypersonic research engine (HRE).

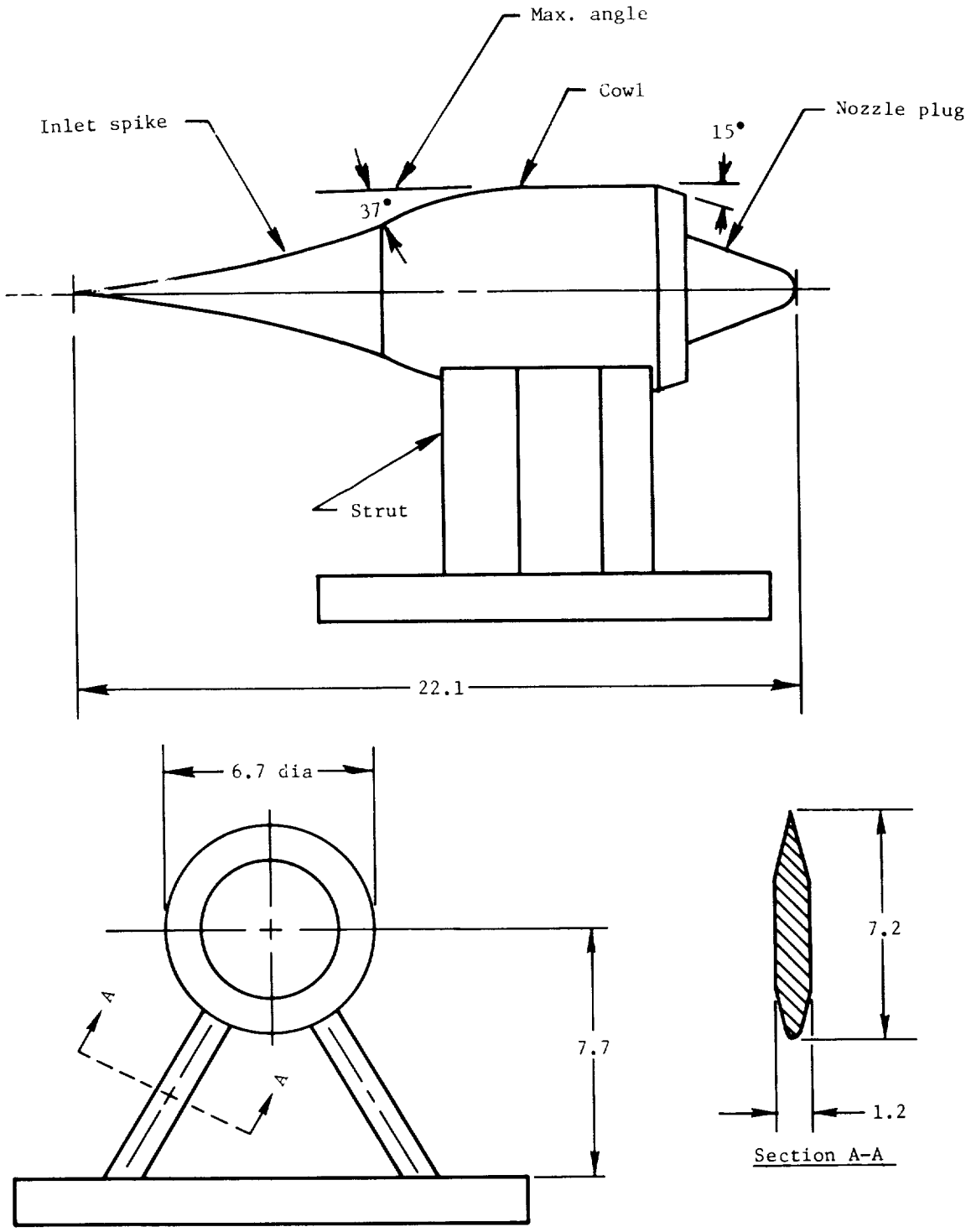

Figure 2.- The HRE model (0.0952 scale). Linear dimensions are in centimeters.

M = 4; D_n = 10.16 cm

Test item	Diam., cm	Percentage of total blockage
Hemisphere	1.27	8.52%
60° Cone	5.08	33.00%
HRE	6.70	48.83%

M = 6 (Ref. 5); D_n = 26.924 cm

Max. blockage allowing flow maintenance

Test item	Diam., cm	Percentage of total blockage
Flat face	7.62	12.02%
Hemisphere	10.16	17.68%
60° Cone	10.16	17.68%

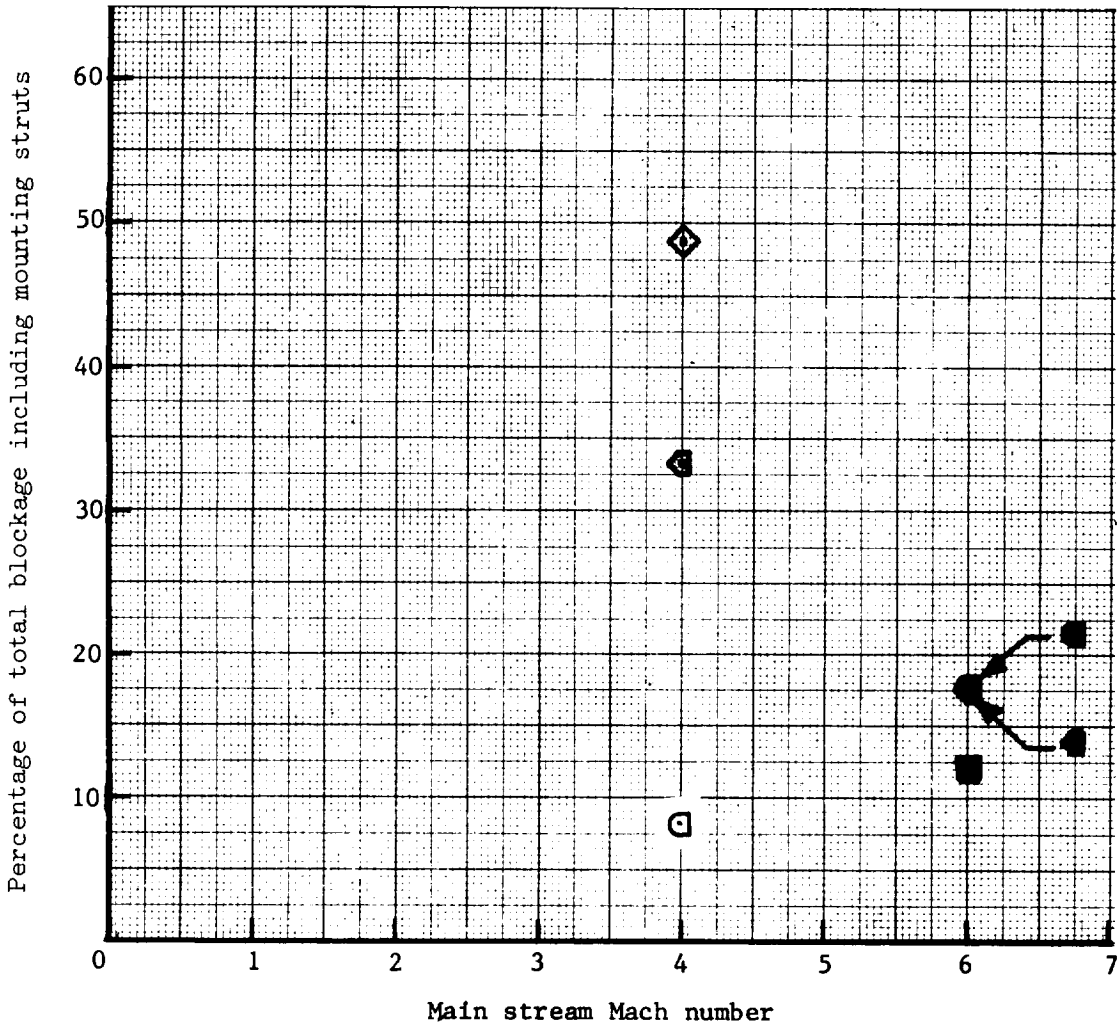

Figure 3.- Mach number versus blockage percent.

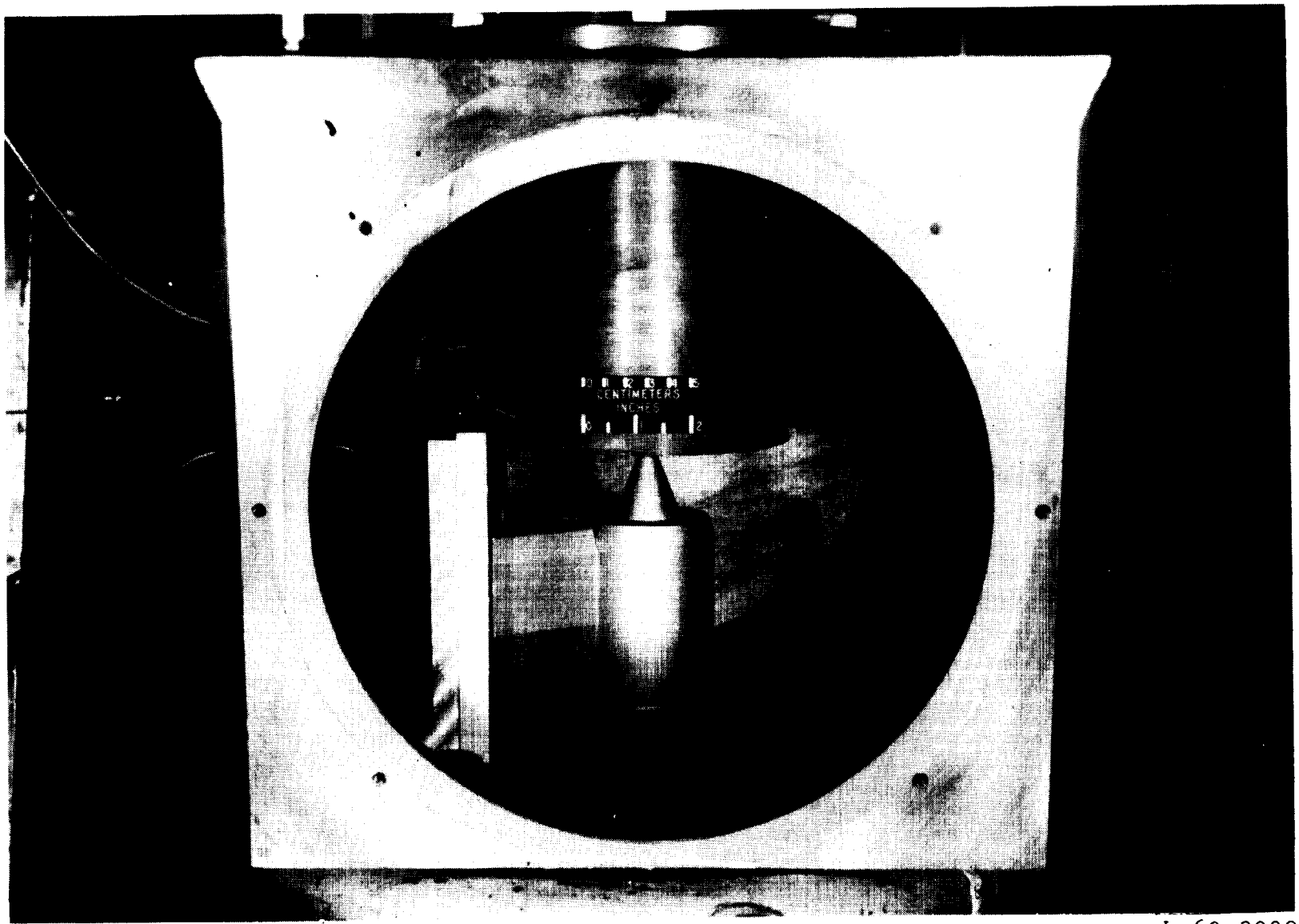

L-69-3992

Figure 4.- The HRE model in fixed position for testing with diffuser configuration 1 and initial free-jet length.

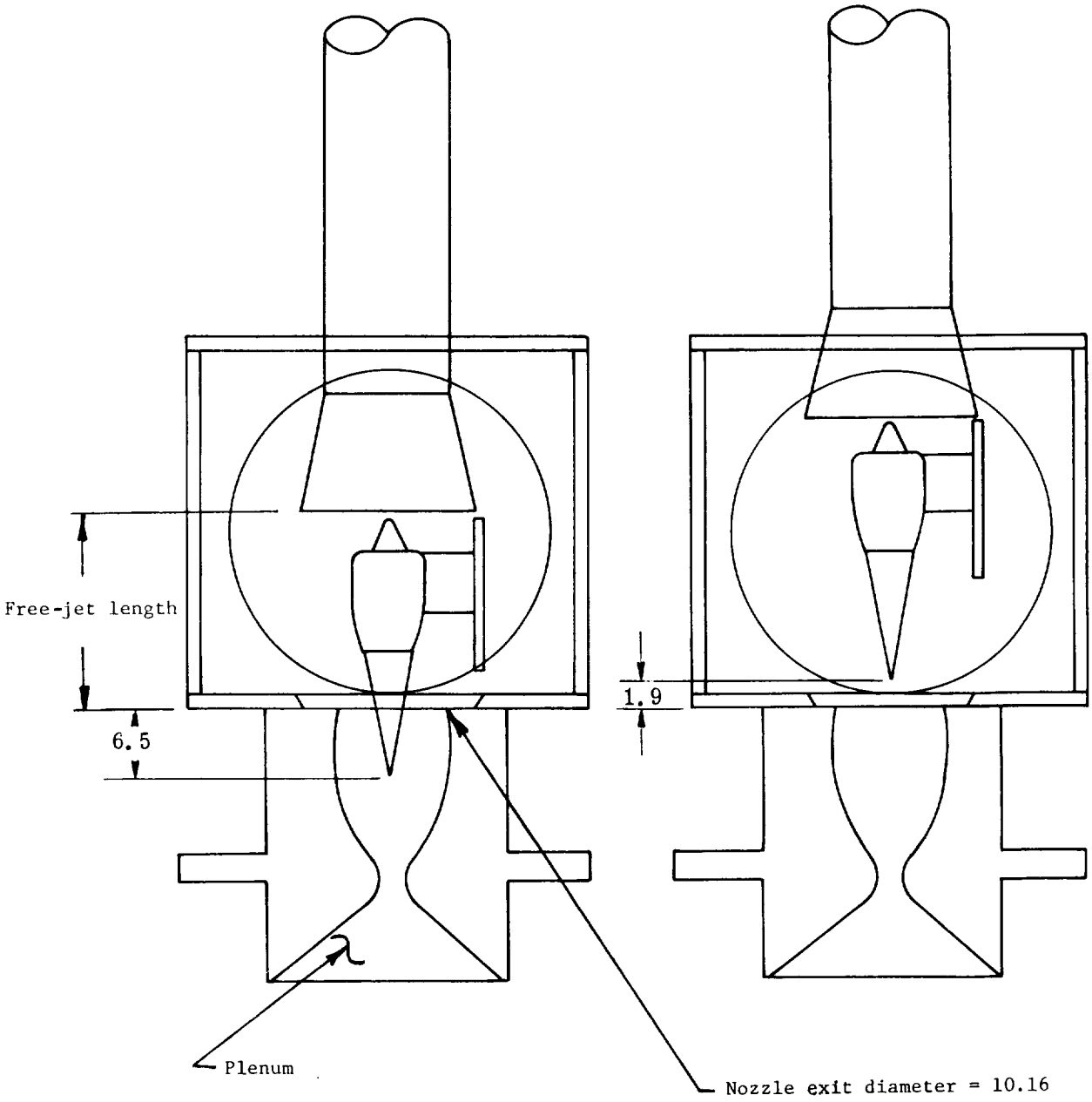

(a) Fixed position. (b) Insertion position.

Figure 5.- The HRE model position in test section.
Dimensions are in centimeters.

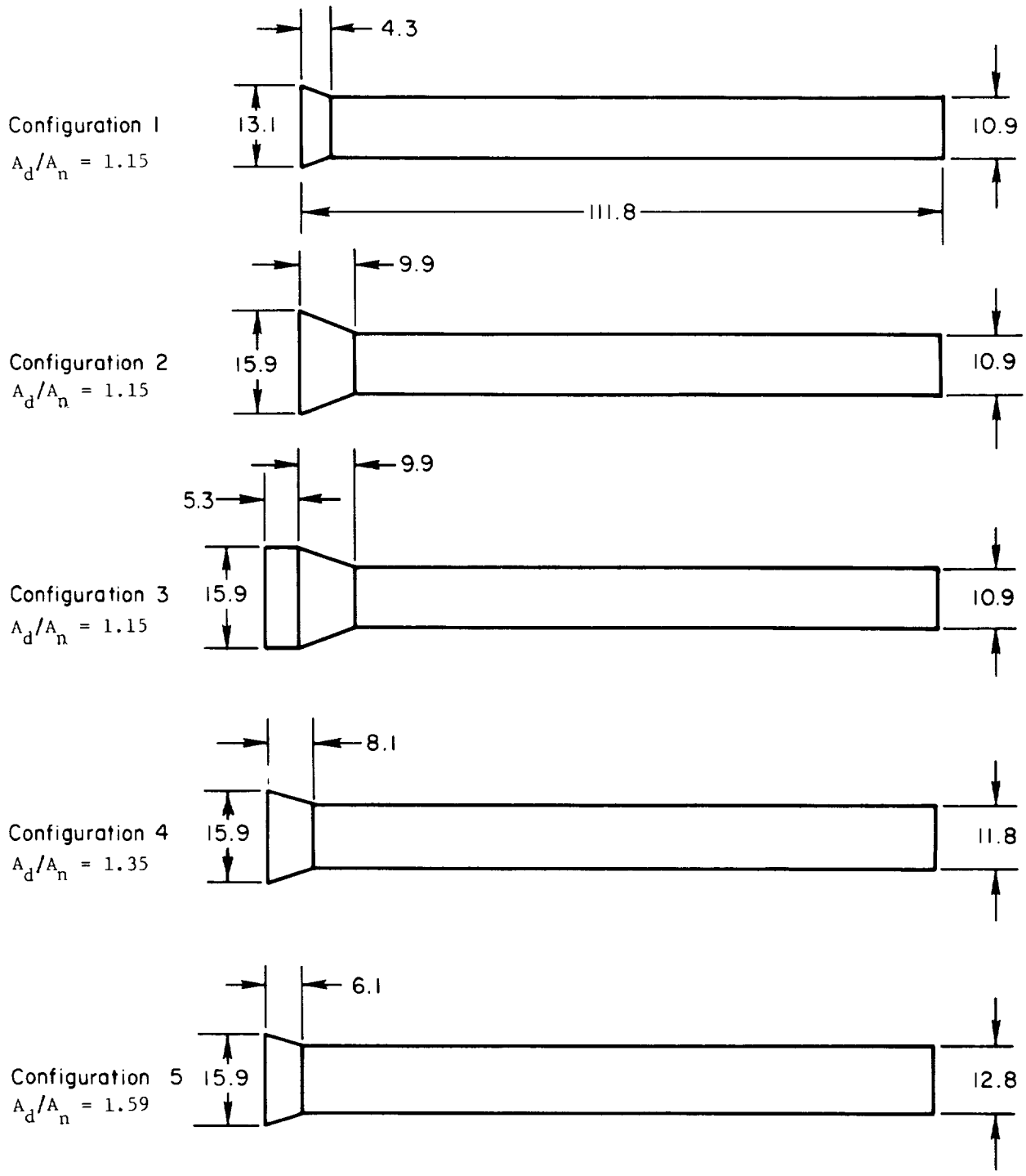

Figure 6.- Diffuser configurations tested. Dimensions are in centimeters.

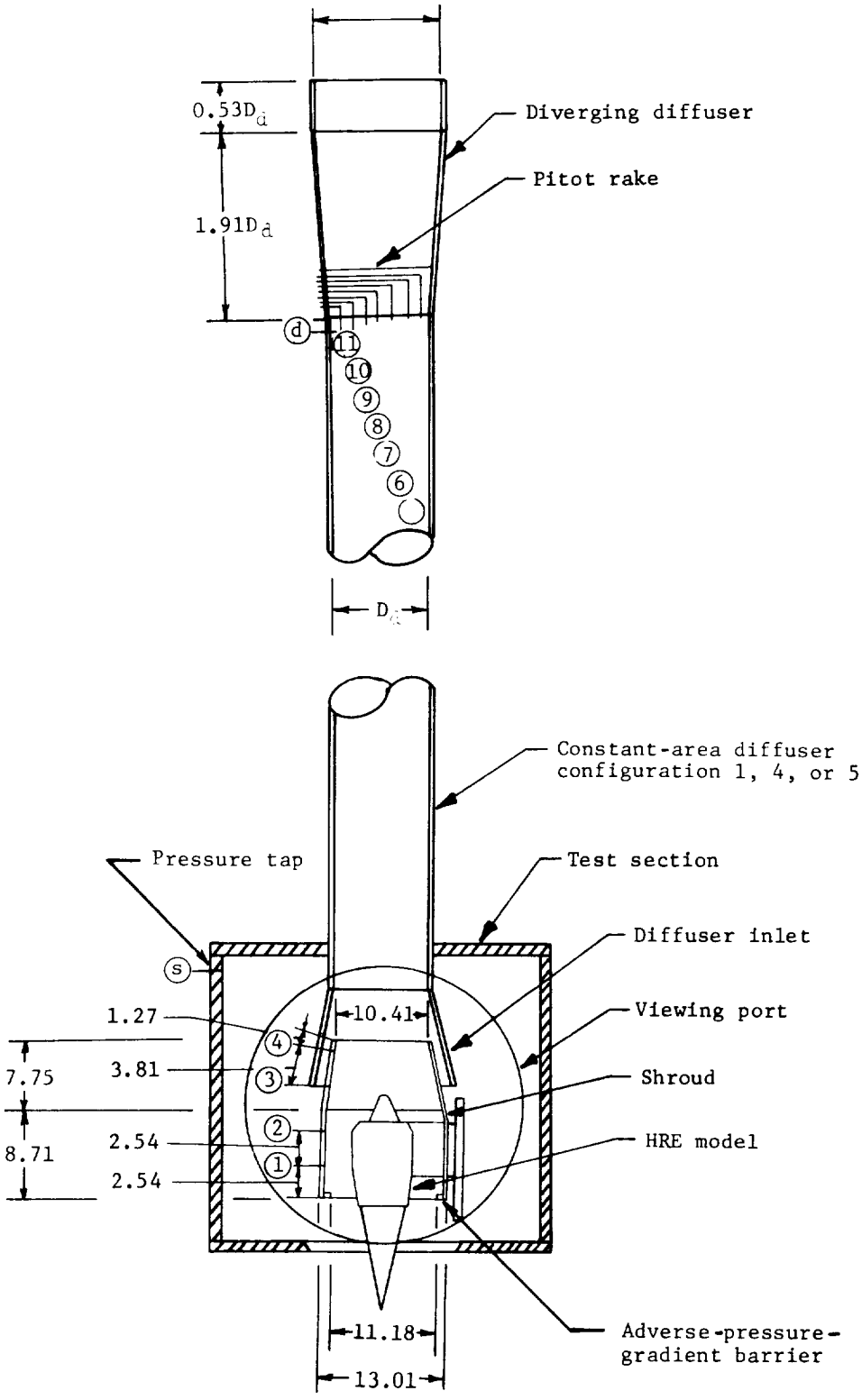

Figure 7.- Arrangement of HRE and HTF model with shroud, diverging diffuser, and pitot rake. Dimensions are in centimeters.

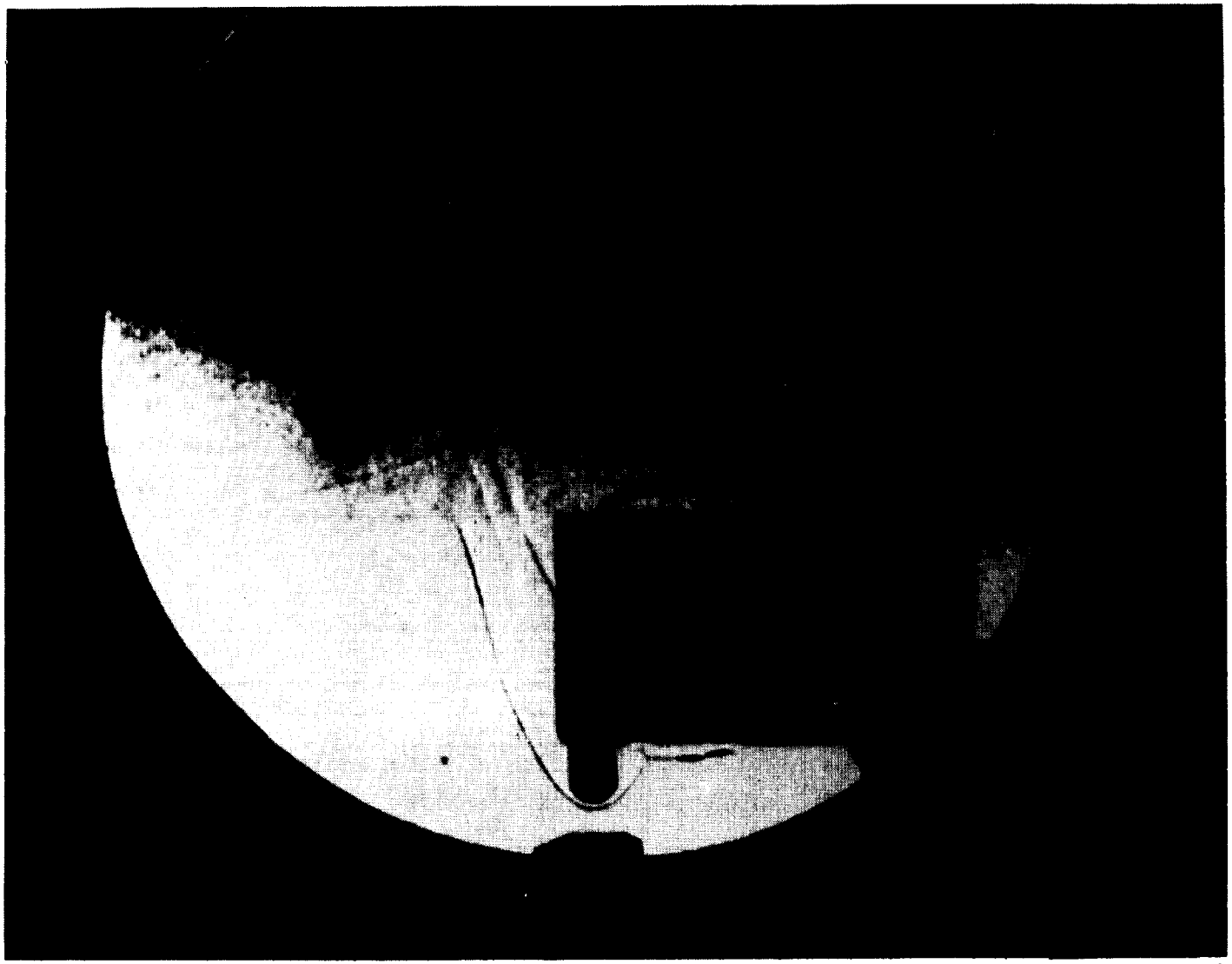

L-76-438

Figure 8.- Shadowgraph of the 1.27-cm-diameter pitot pressure probe showing established flow conditions with the tunnel started.

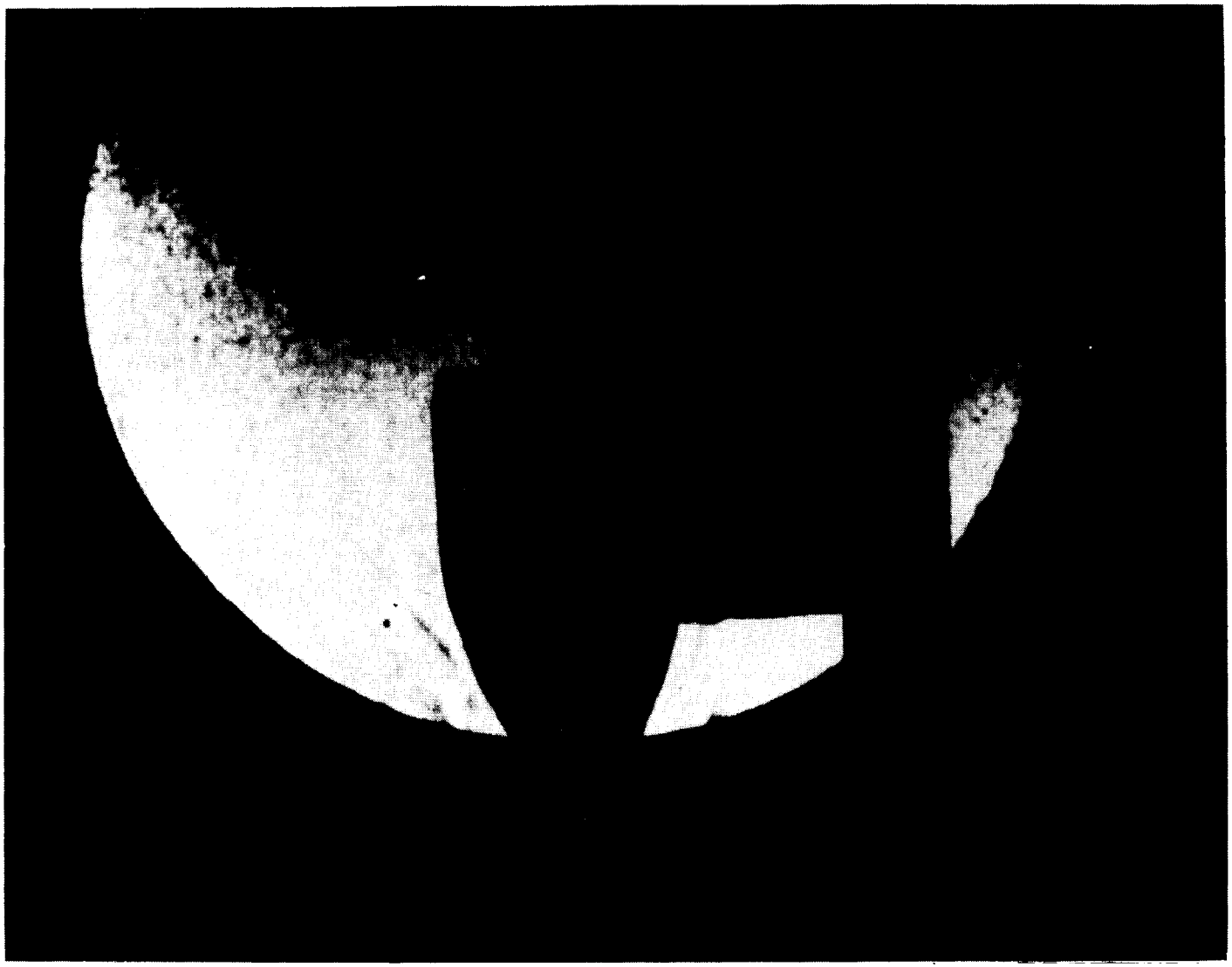

L-76-439

Figure 9.- Shadowgraph of the HRE model with tunnel unstarted.

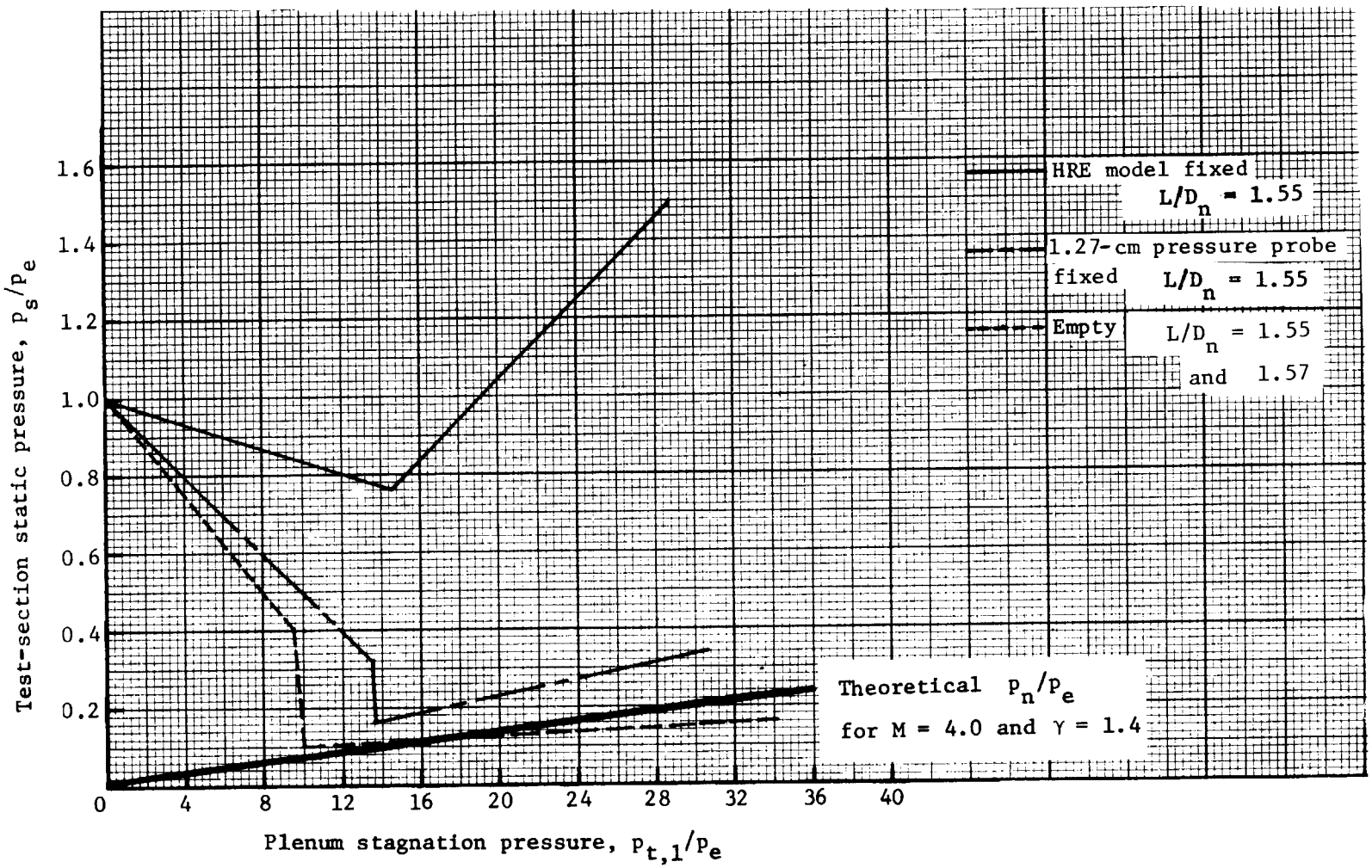

Figure 10.- Variation of test-section static pressure with plenum stagnation pressure for diffuser configuration 1.

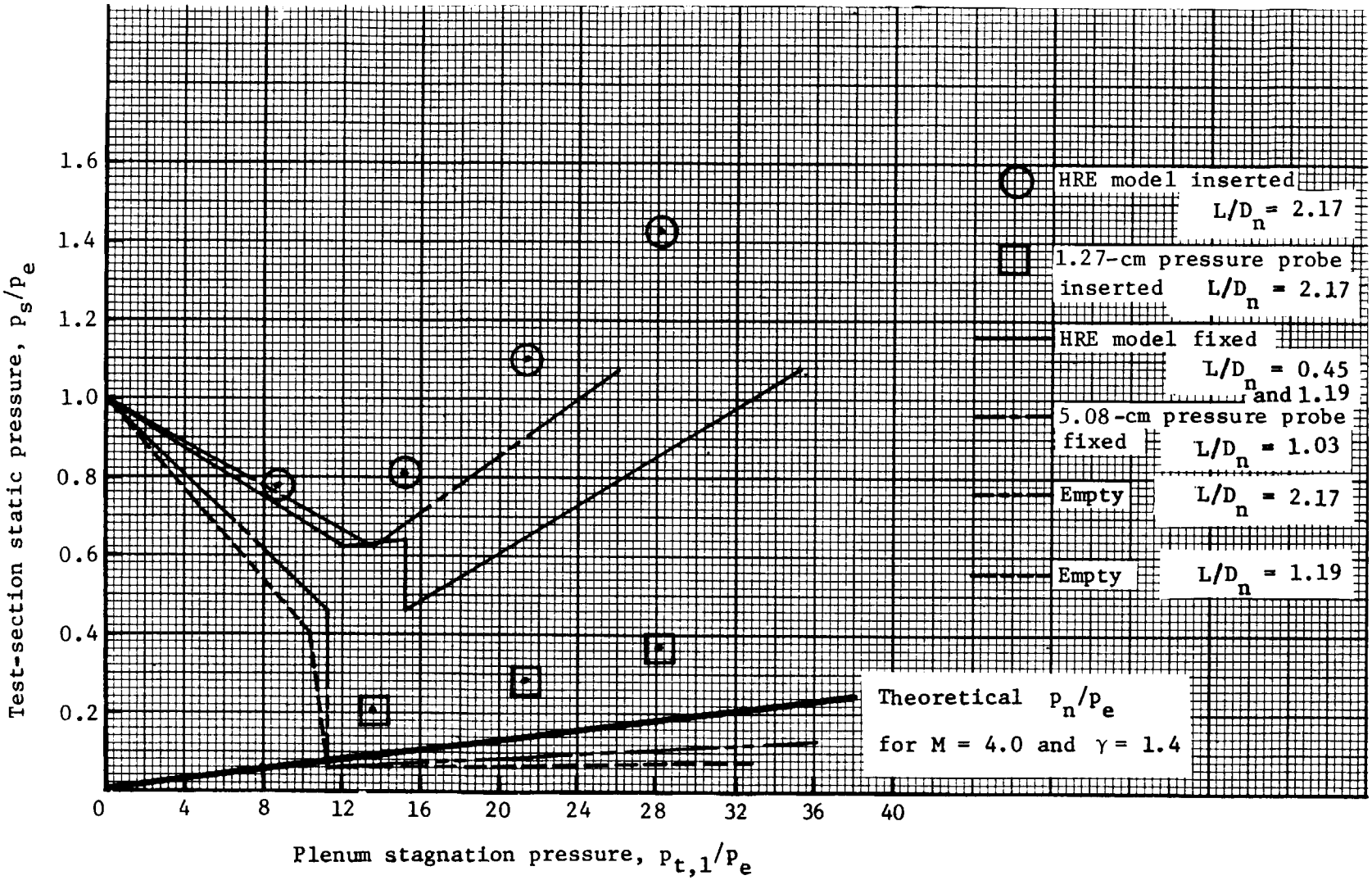

Figure 11.- Variation of test-section static pressure with plenum stagnation pressure for diffuser configuration 2.

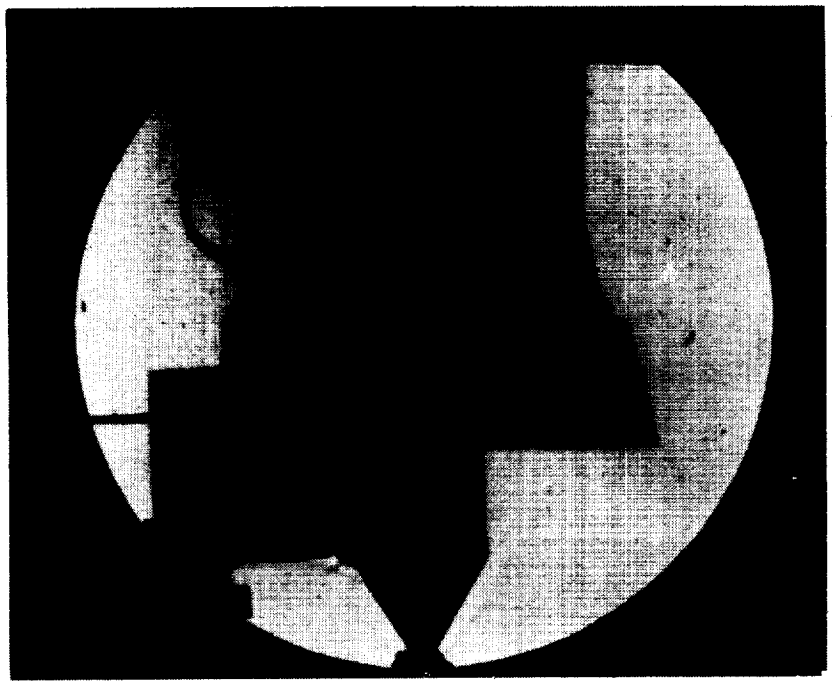

L-76-616

Figure 12.- Shadowgraph of the 5.08-cm-diameter pitot pressure probe with the tunnel unstarted.

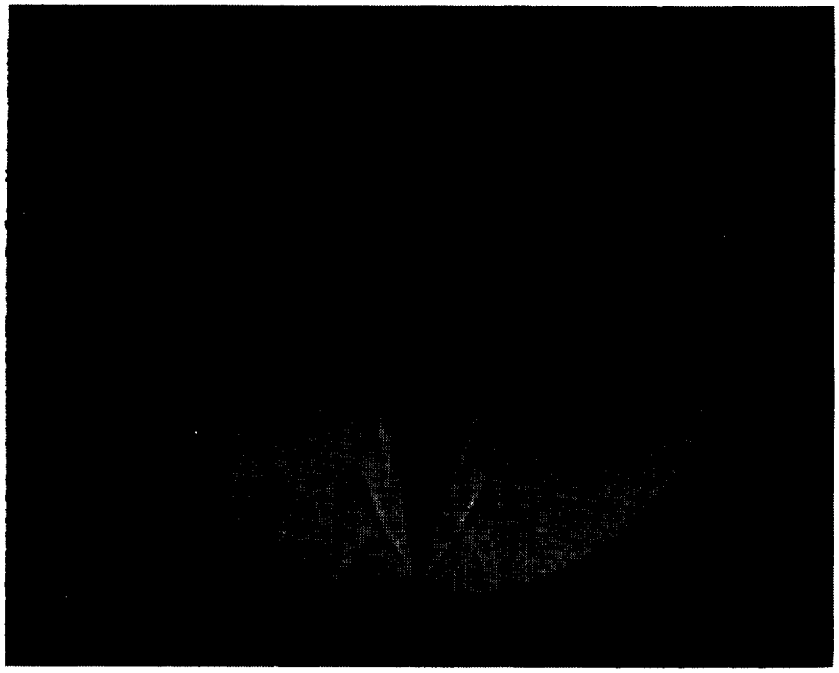

L-76-441

Figure 13.- Shadowgraph of the tunnel unstarted after insertion of the HRE model, causing disturbed flow.

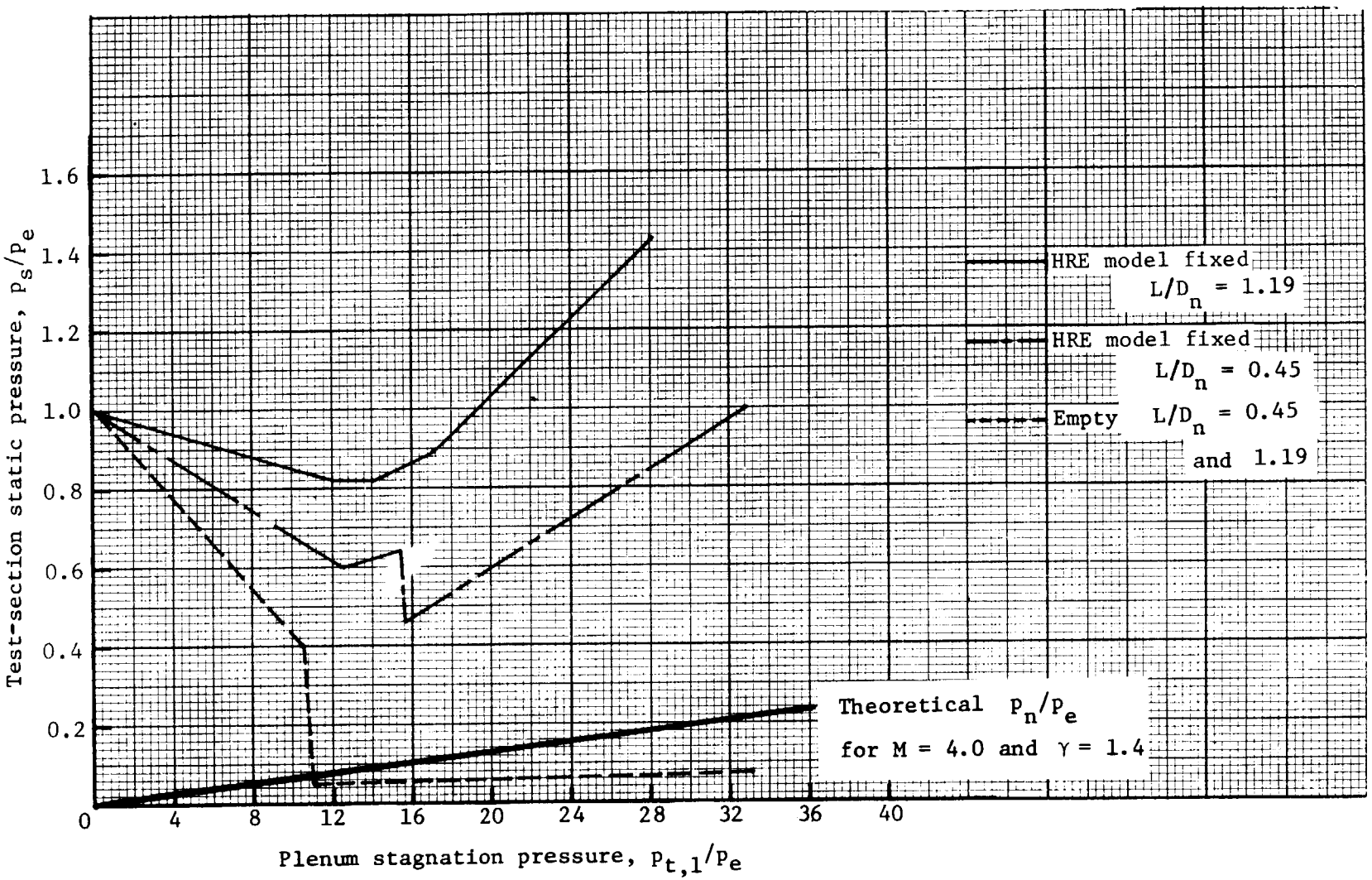

Figure 14.- Variation of test-section static pressure with plenum stagnation pressure for diffuser configuration 3.

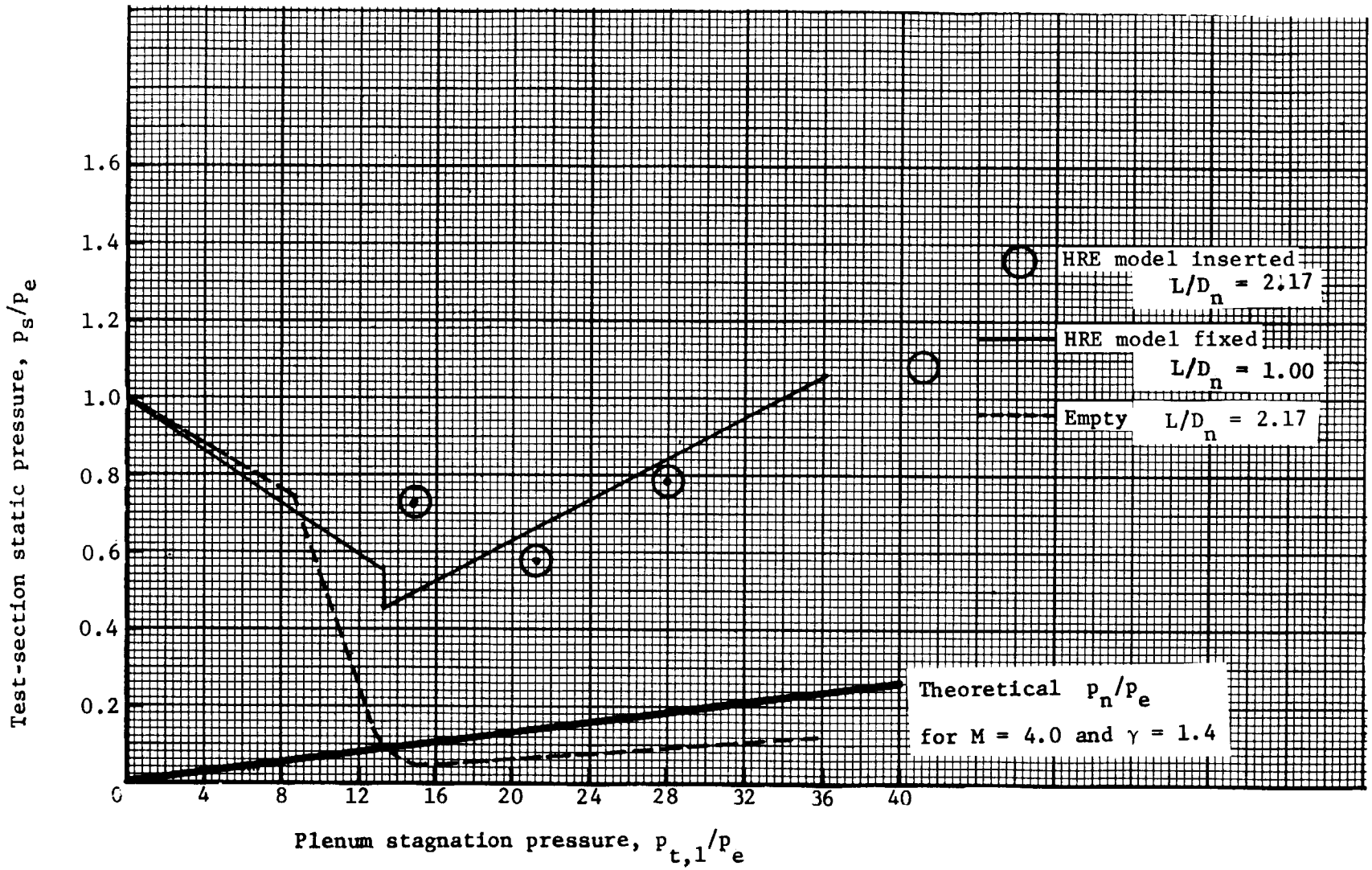

Figure 15.- Variation of test-section static pressure with plenum stagnation pressure for diffuser configuration 4.

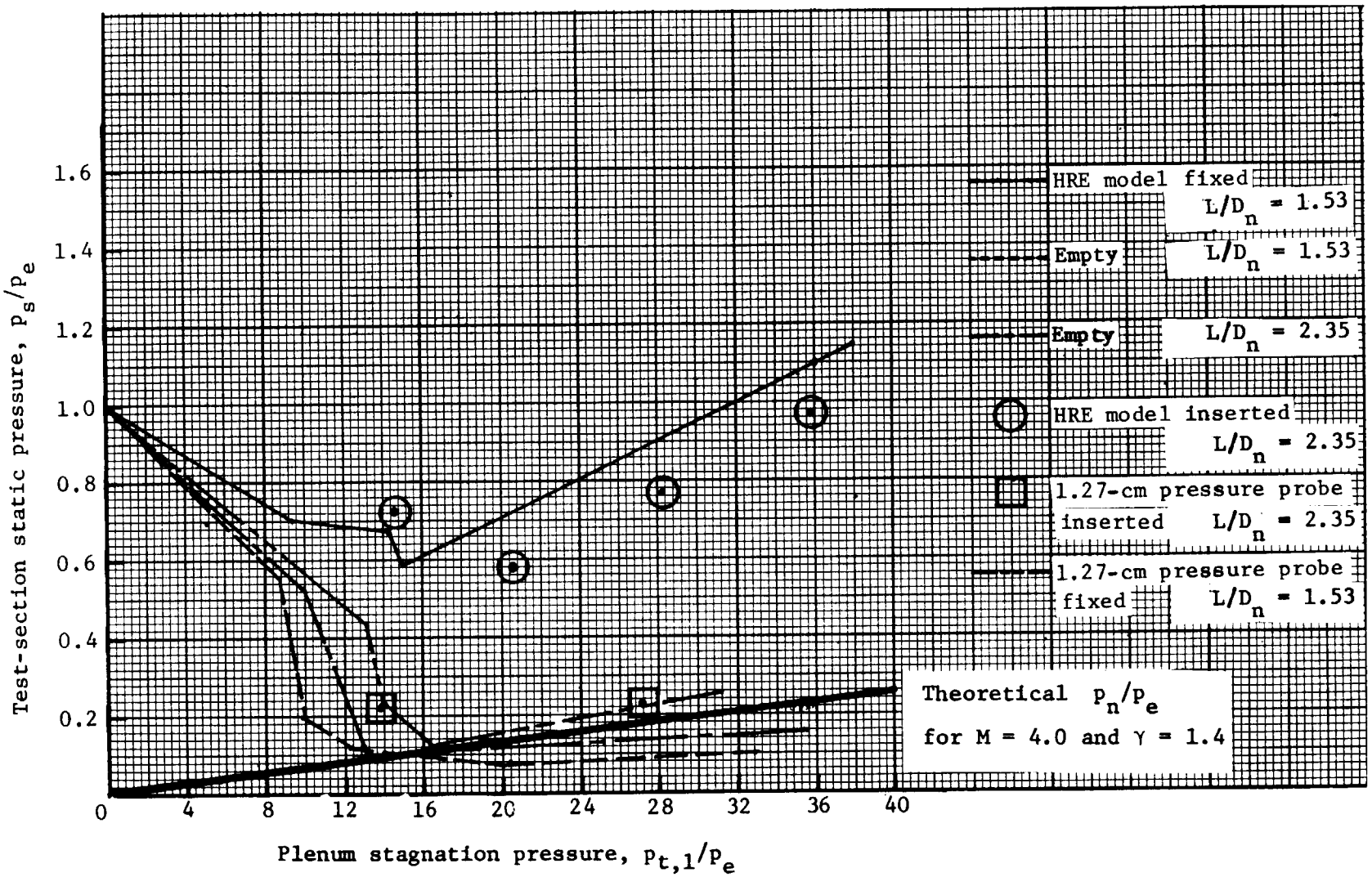

Figure 16.- Variation of test-section static pressure with plenum stagnation pressure for diffuser configuration 5.

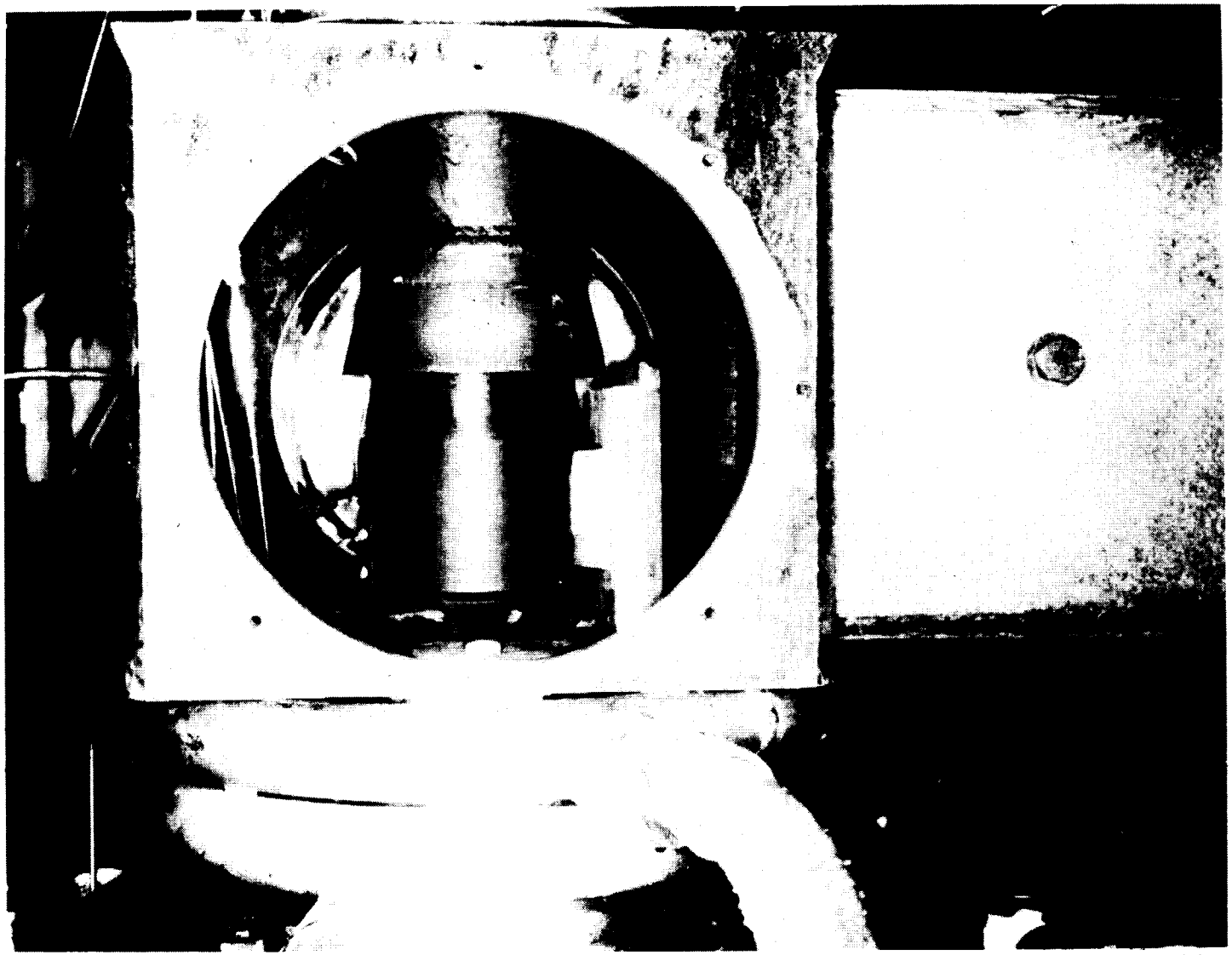

L-76-442

Figure 17.- The HRE model with shroud installed in test section.

L-70-4562

Figure 18.- Forward view of the HRE model with shroud.

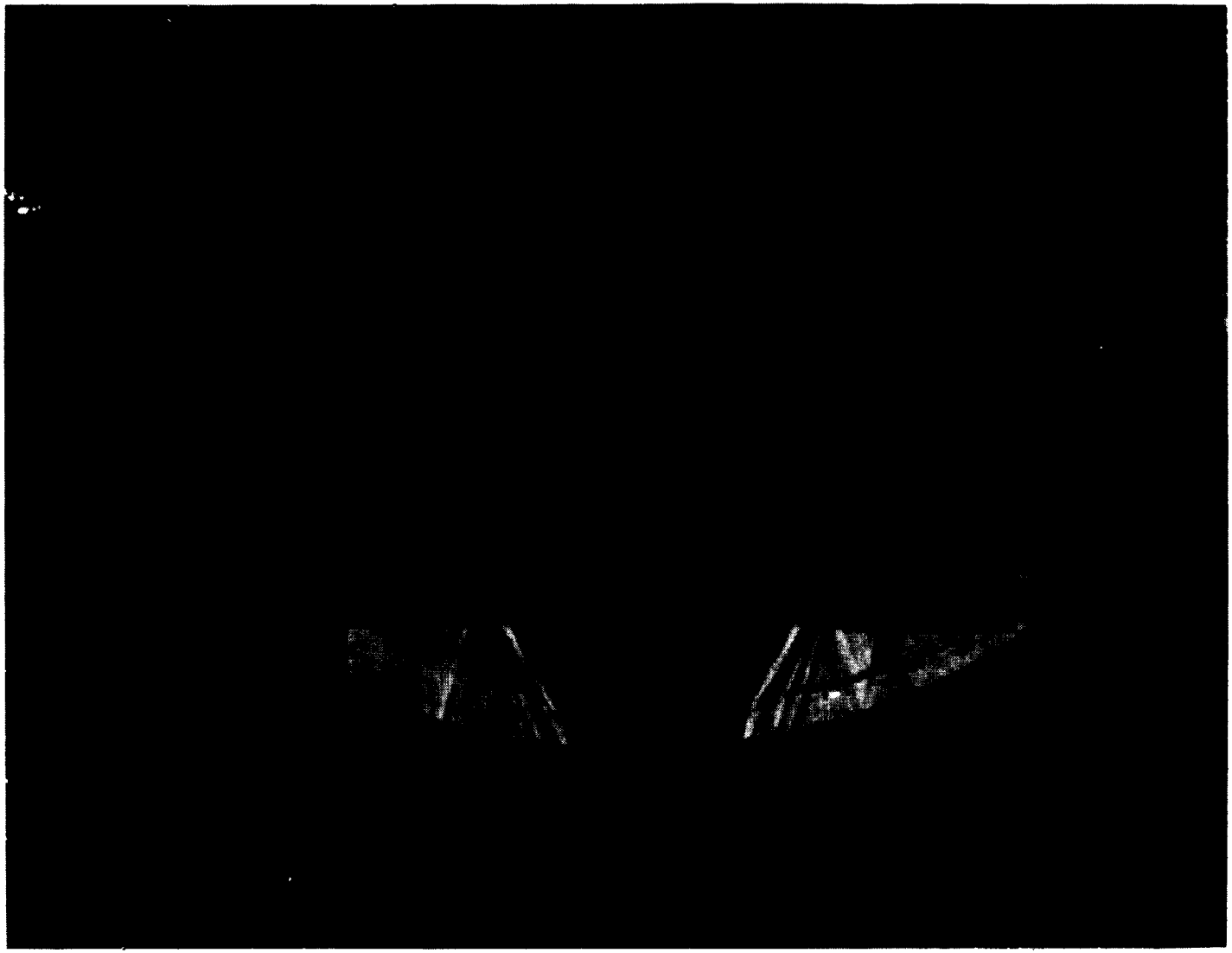

L-76-440

Figure 19.- Shadowgraph of the HRE model with shroud and the tunnel started.

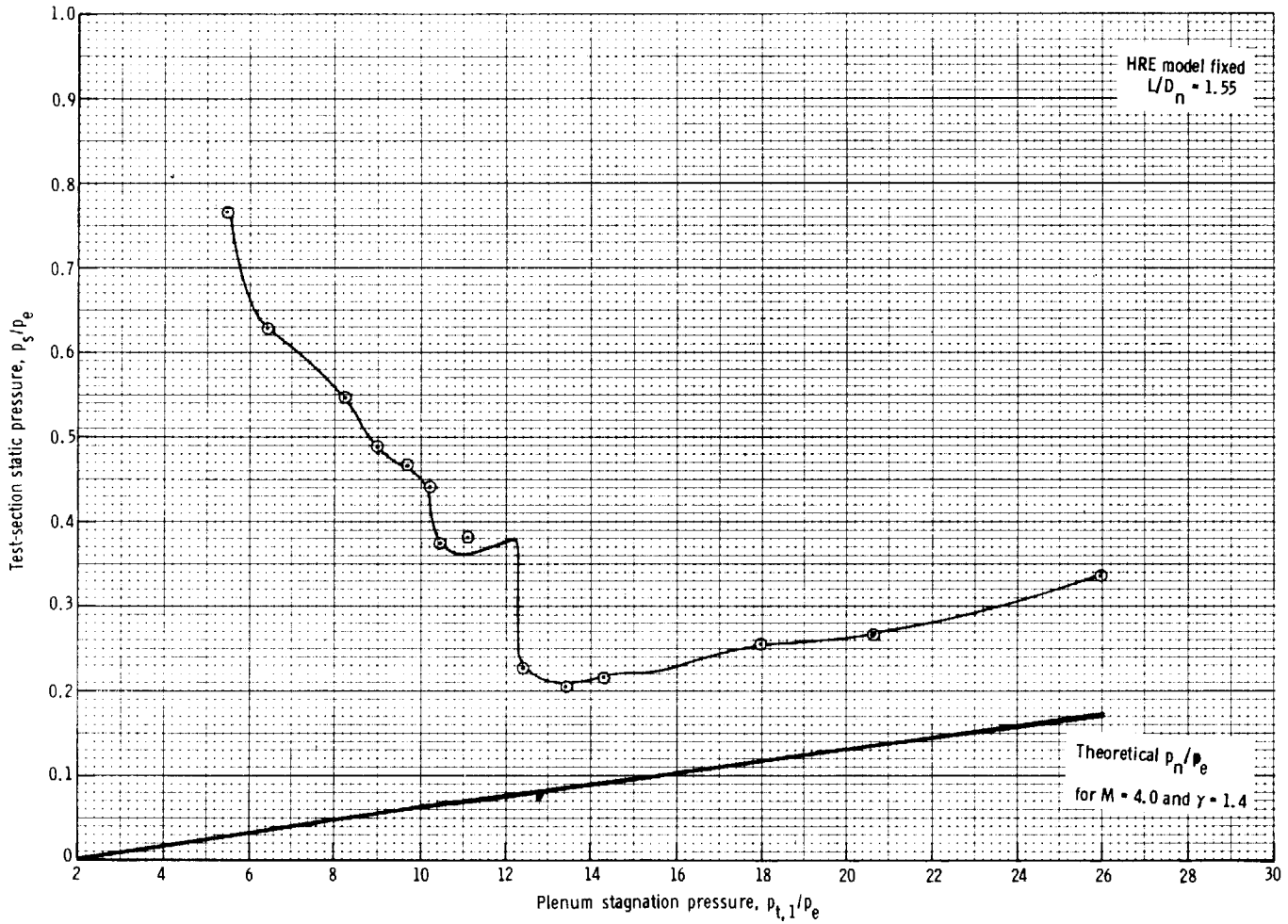

Figure 20.- Variation of test-section static pressure with plenum stagnation pressure for the HRE model with shroud and diffuser configuration 1.

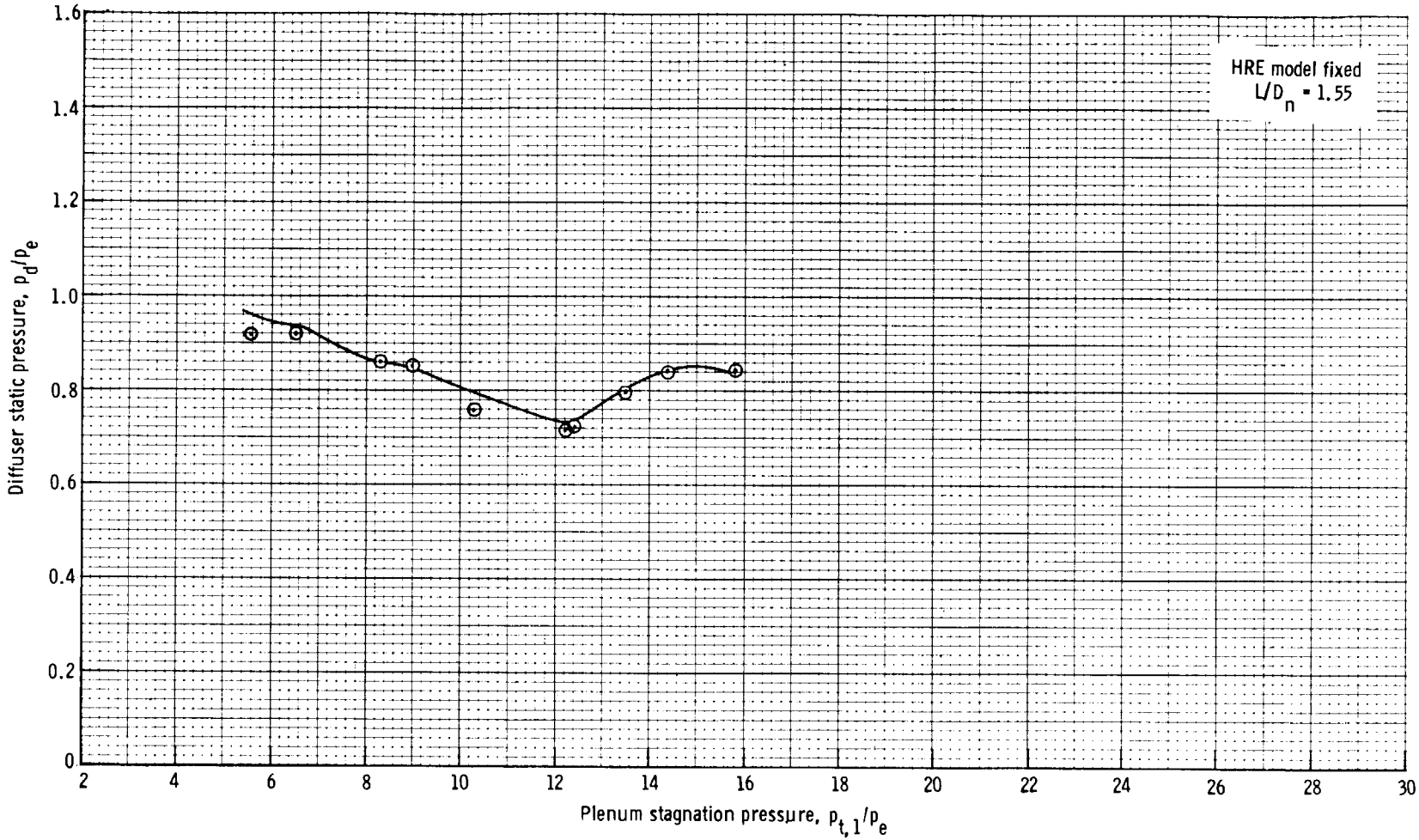

Figure 21.- Variation of diffuser static pressure with plenum stagnation pressure for the HRE model with shroud and diffuser configuration 1.

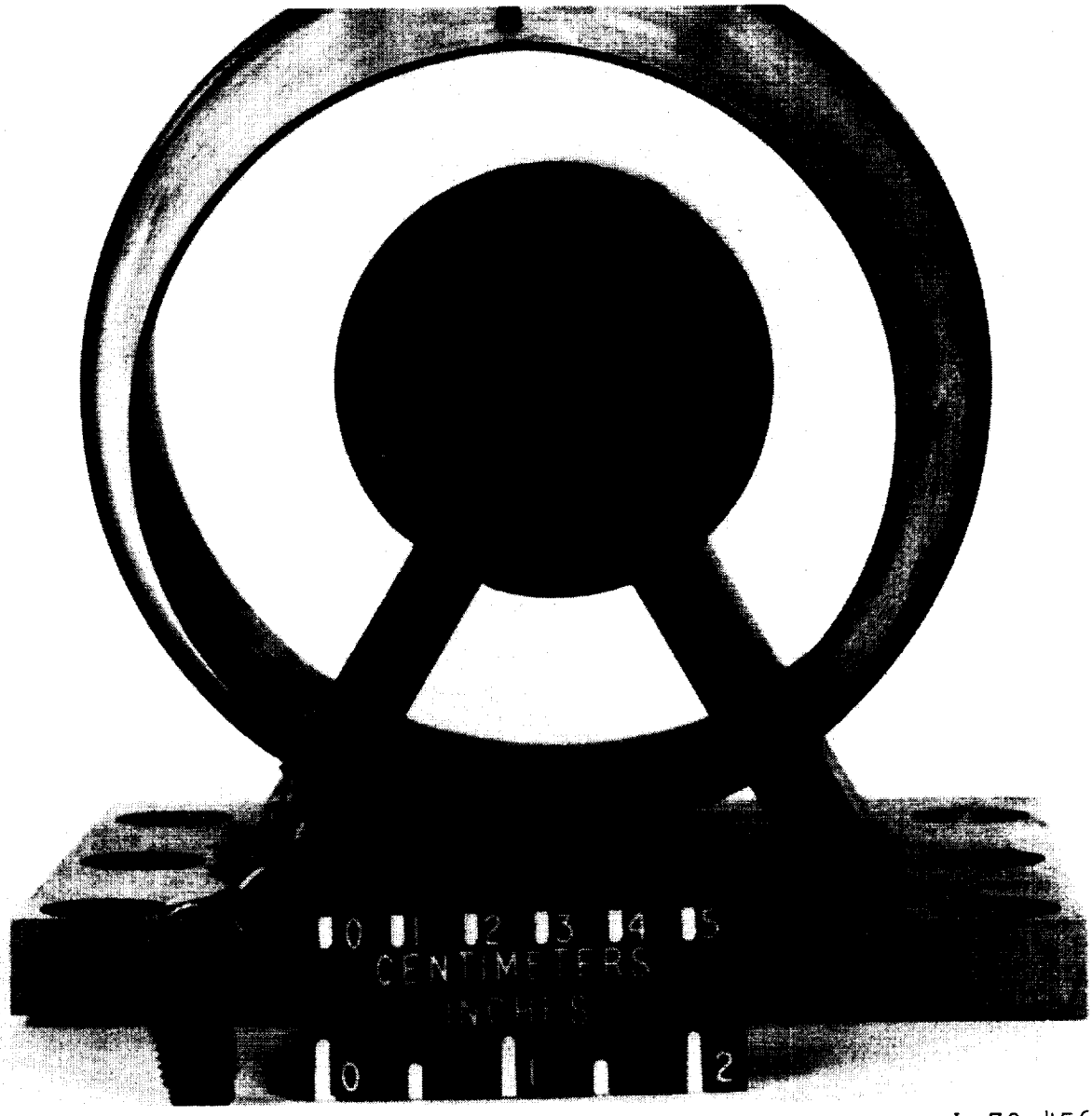

L-70-4561

Figure 22.- Aft view of the HRE model with shroud and simulated instrumentation-cooling-water discharge system.

L-70-5265

Figure 23.- Forward view of the HRE model with shroud, simulated instrumentation-cooling-water discharge system, and adverse-pressure-gradient barrier.

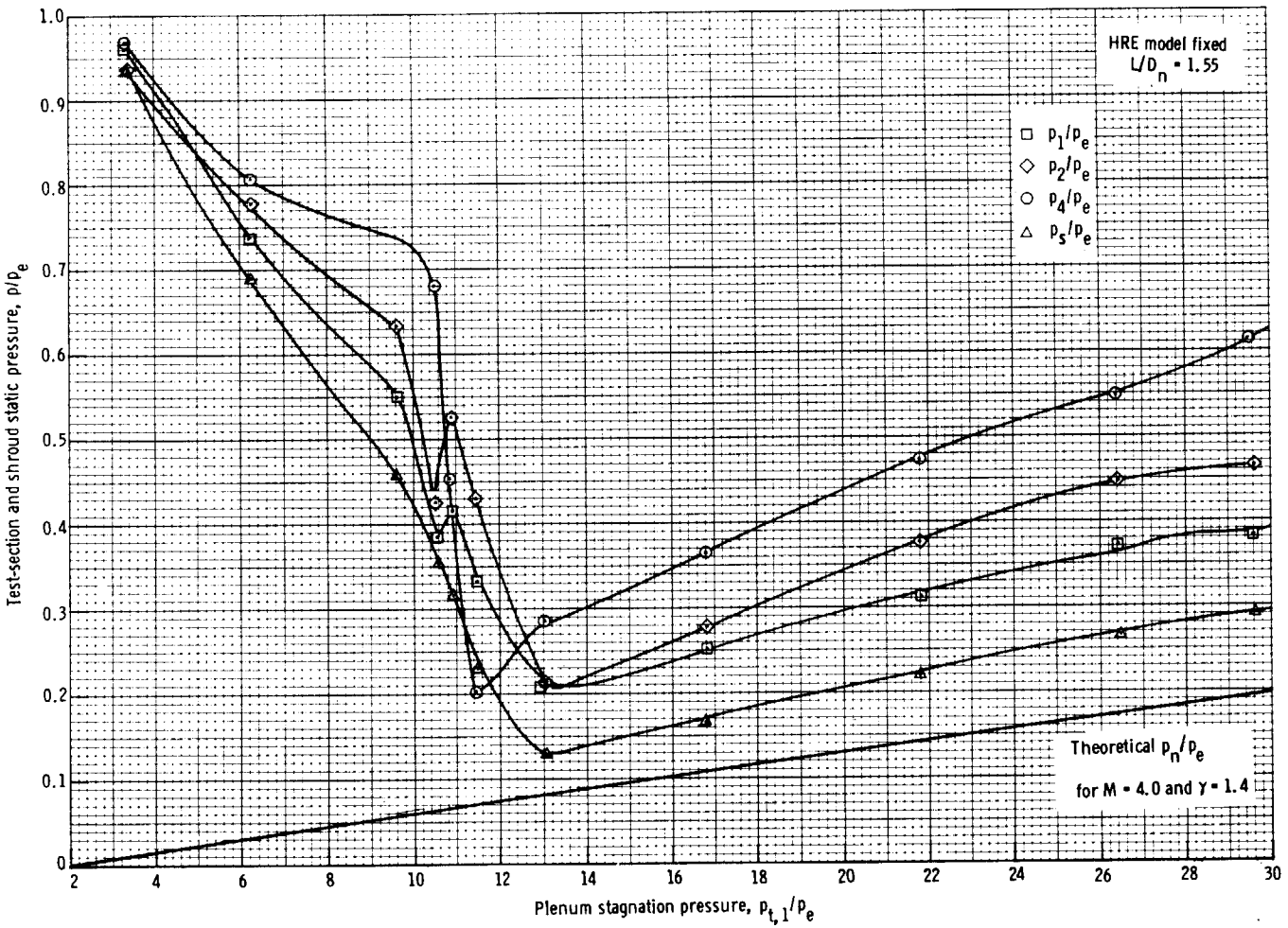

Figure 24.- Variation of test-section and shroud pressure with stagnation pressure for the HRE model with shroud, barrier, and water injection (0.136 kg/s) diffuser configuration 1.

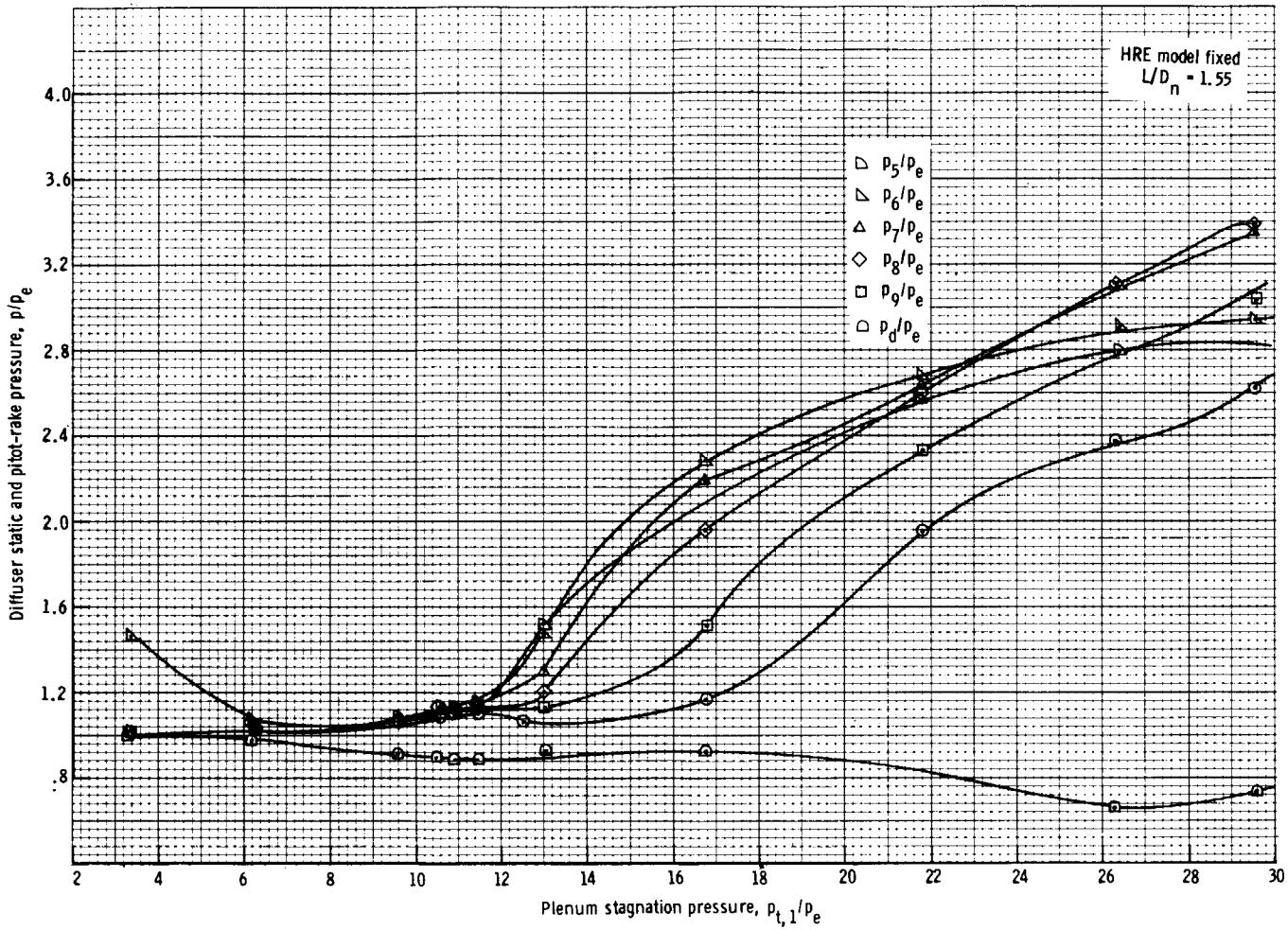

Figure 25.- Variation of diffuser static and pitot-rake pressure with plenum stagnation pressure for the HRE model with shroud, barrier, and water injection (0.136 kg/s) for diffuser configuration 1.

L-70-5266

Figure 26.- Aft view of the HRE model with shroud, adverse-pressure-gradient barrier, and simulated airflow metering duct.

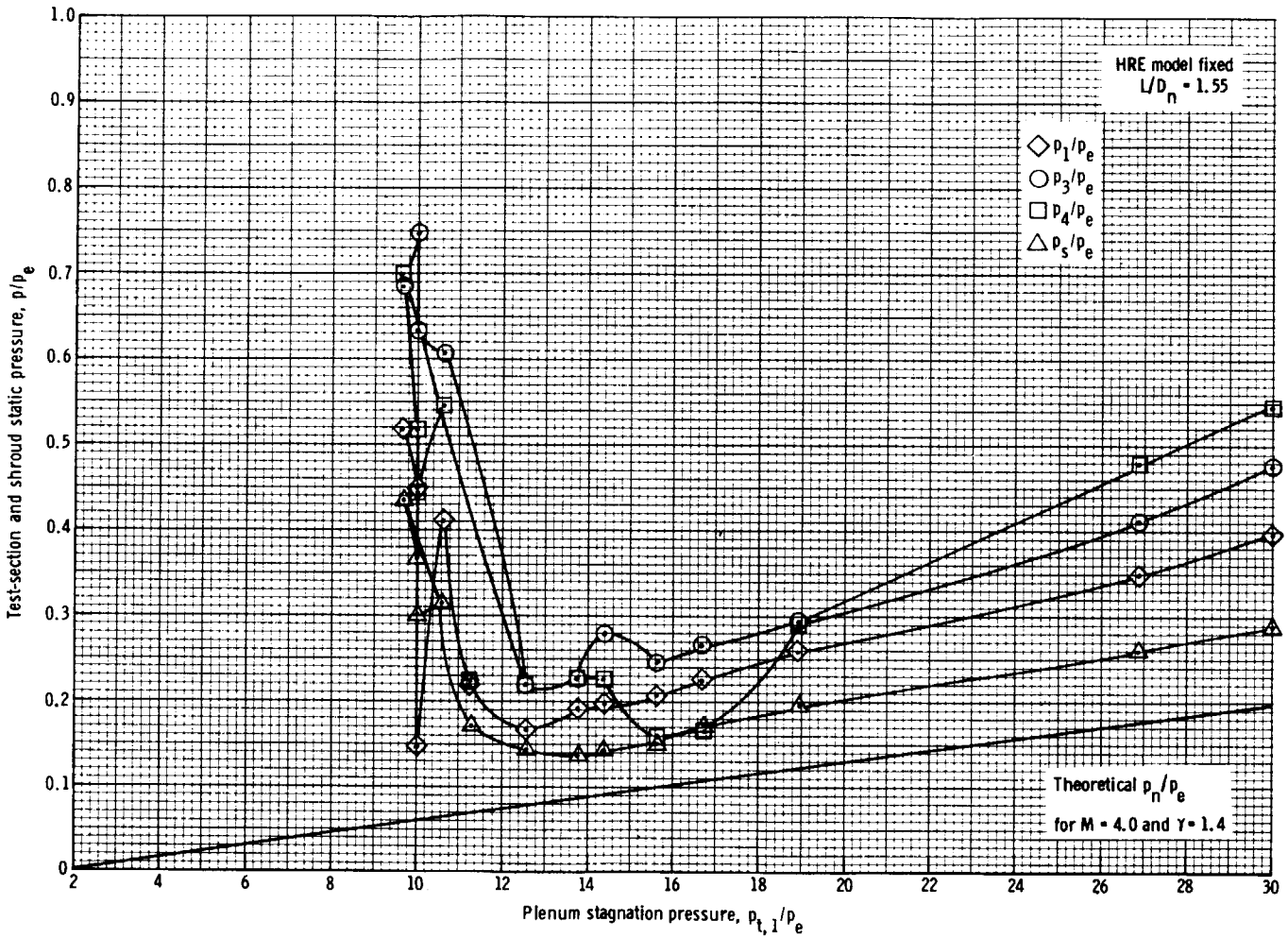

Figure 27.- Variation of test-section and shroud static pressure with stagnation pressure for the HRE model with shroud, barrier, and airflow metering duct for diffuser configuration 1.

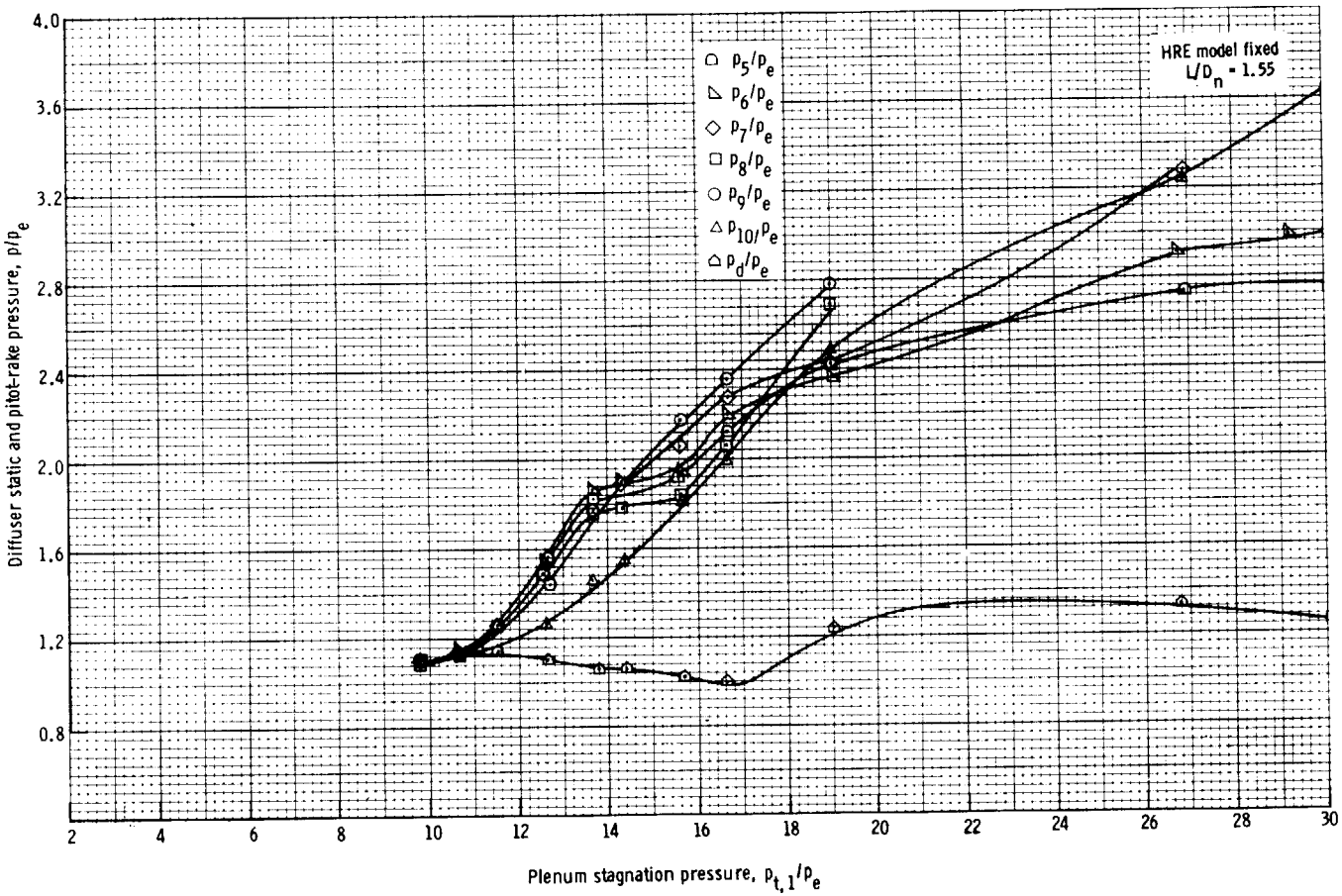

Figure 28.- Variation of diffuser static and pitot-rake pressure with plenum stagnation pressure for the HRE model with shroud, barrier, and airflow metering duct for diffuser configuration 1.

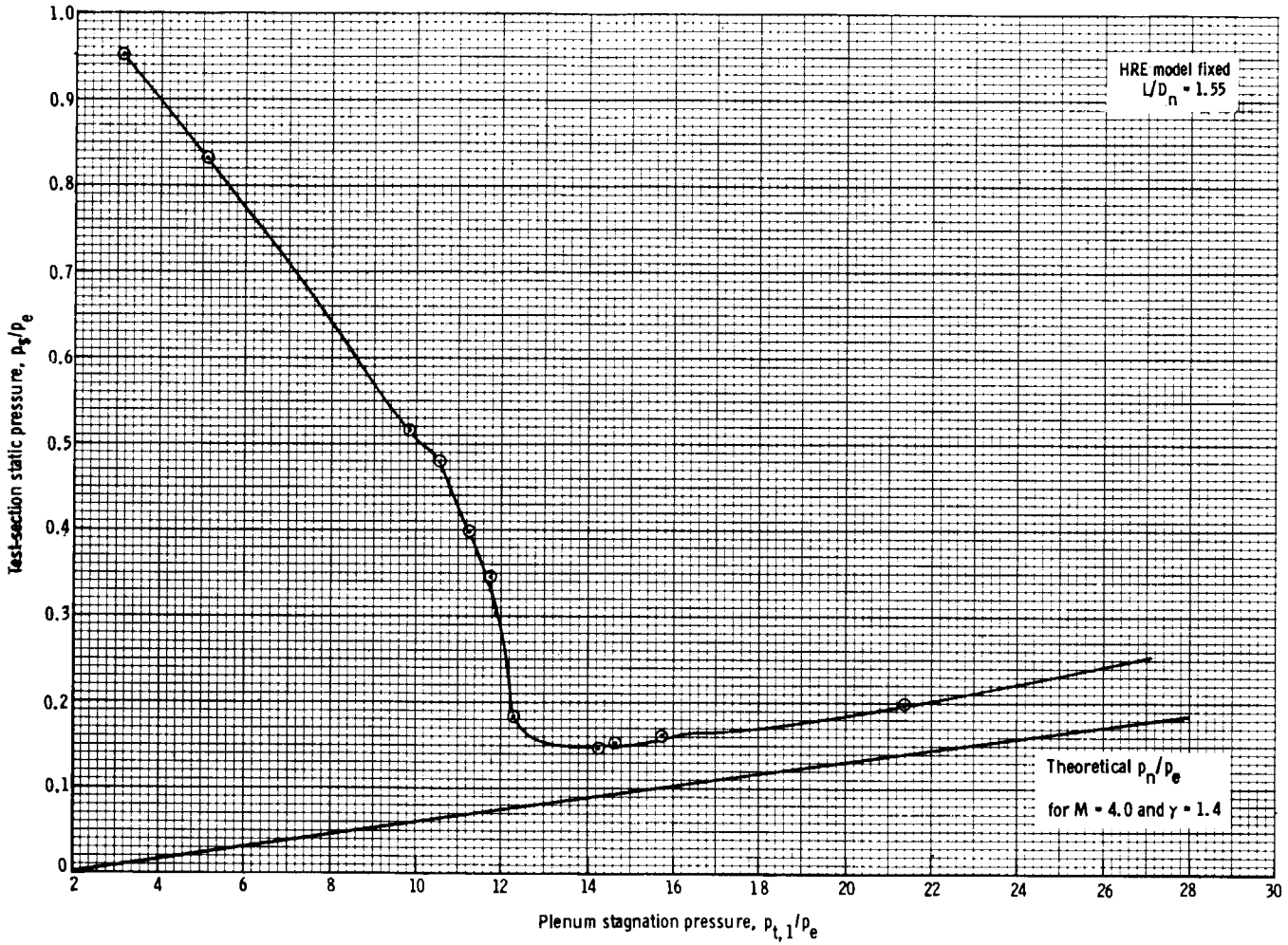

Figure 29.- Variation of test-section static pressure with stagnation pressure for the HRE model with shroud, barrier, and airflow metering duct for diffuser configuration 4.

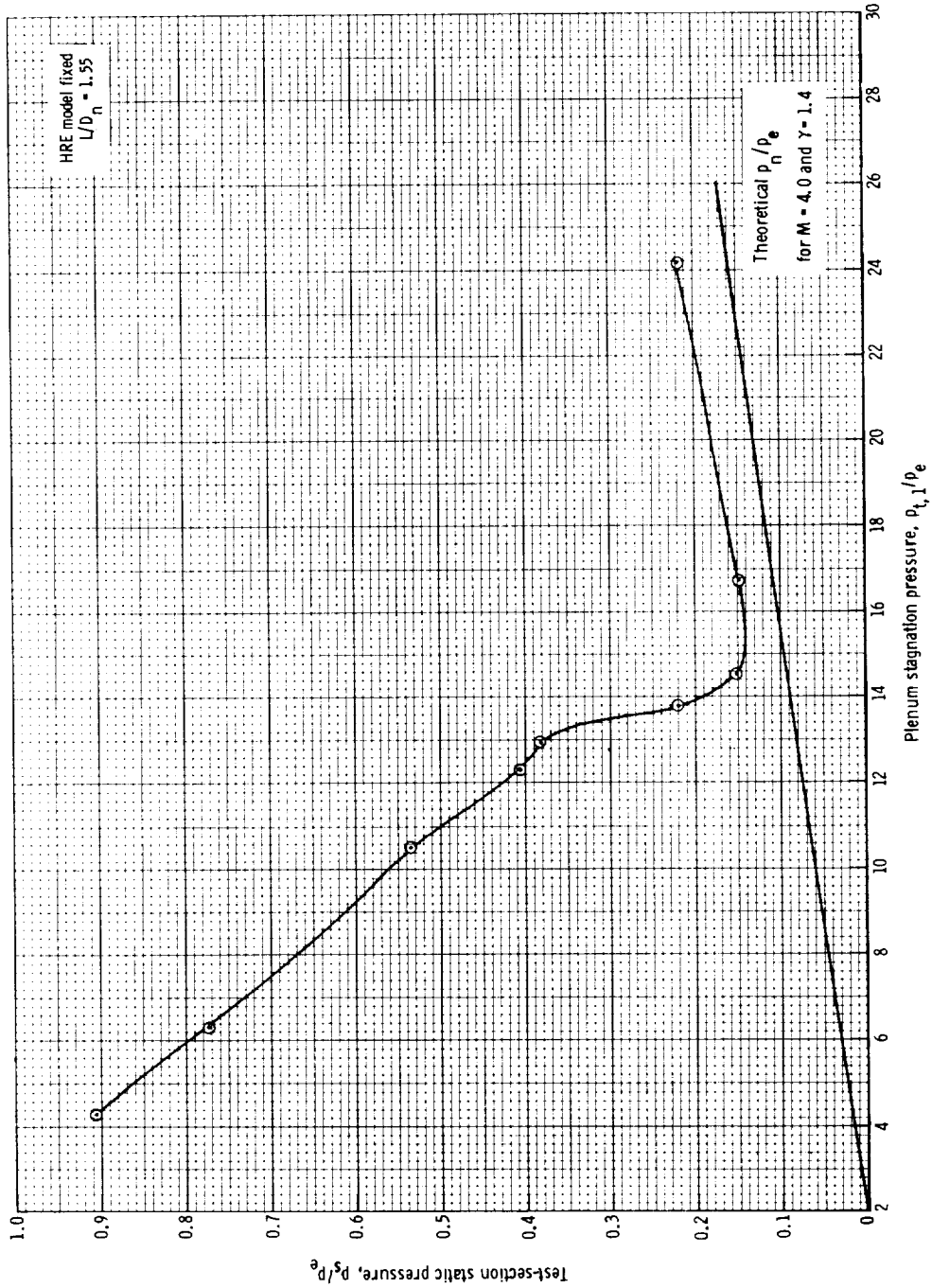

Figure 30.- Variation of test-section static pressure with stagnation pressure for the HRE model with barrier and airflow metering duct for diffuser configuration 5.

NASA-Langley, 1976 L-10525